Experimental study of eutectogels for drug delivery

TESI DI LAUREA MAGISTRALE IN
BIOMEDICAL ENGINEERING
INGEGNERIA BIOMEDICA

Author: **Joanna Pietrowska**

Student ID: 942835
Advisor: Professor Franca Castiglione
Co-advisor: Valeria Vanoli
Academic Year: 2023-24

Abstract

Due to the need to improve current solutions for controlled drug delivery to treat an ever-increasing number of injuries and diseases, novel supramolecular eutectogels loaded with ethosuximide have been proposed. Eutectogels, made of menthol and thymol, were prepared with 2 different weight contents of gelling agent – 1,3:2,4-dibenzylidene-D-sorbitol (DBS). The drug was loaded at three different concentrations. The analytical characterization of the gels included the study of the morphology with SEM technique, the investigation of the intermolecular interactions between the eutectogel components and the drug, using FT-IR technique. Moreover, High-Resolution Magic Angle Spinning (HR-MAS) NMR Spectroscopy has been used to investigate the transport behaviour of the drug, menthol, and thymol inside the 3D gel network. Finally, *in vitro* drug release study has been performed under different experimental conditions, such as different temperatures and different pHs. The obtained results confirmed the thermo-responsive and pH-responsive character of eutectogels, proving that different environments influence the strength of hydrogen bonds inside the structure. The mass of drug released was also dependent on the quantity of gelator, as higher values of drug release were observed from gels prepared with lower DBS content. The results allow concluding that the obtained eutectogels are a good system for the controlled release of ethosuximide, which occurs through a quasi-Fickian diffusion mechanism.

Key-words: Eutectogels, Ethosuximide, Drug delivery, Diffusion, HR-MAS NMR

Abstract in italiano

Lo studio di eutectogel supramolecolari con etosuccimide incapsulato all'interno nasce dalla necessità di migliorare le attuali soluzioni per la somministrazione controllata di farmaci per il trattamento di un numero sempre crescente di lesioni e malattie. Gli eutectogels, a base di mentolo e timolo, sono stati preparati con 2 diversi contenuti in peso di agente gelificante – 1,3:2,4-dibenzilidene-D-sorbitolo (DBS). Il farmaco è stato caricato a 3 diverse concentrazioni. La caratterizzazione analitica concerne la morfologia dei gels con la tecnica SEM, lo studio delle interazioni intermolecolari tra i componenti dell'eutectogel e il farmaco utilizzando la tecnica FT-IR. La Spettroscopia NMR ad Angolo Magico ad Alta Risoluzione (HR-MAS) è stata utilizzata per studiare i fenomeni di trasporto del farmaco, mentolo e timolo nella struttura 3D del gel. Infine, lo studio *in vitro* della cinetica di rilascio del farmaco è stato condotto in diverse condizioni sperimentali con diverse temperature e diversi condizioni di pH. I risultati ottenuti hanno confermato il carattere termo-responsivo e pH-responsivo degli eutectogels, dimostrando che ambienti diversi influenzano la forza dei legami a idrogeno all'interno della struttura tridimensionale dei gels. La massa di farmaco rilasciata dipende anche dalla quantità di agente gelificante usato nella preparazione del gel; infatti, sono stati osservati valori più alti di rilascio da gels preparati con un contenuto inferiore di DBS. I risultati ottenuti consentono di concludere che entrambe le formulazioni di eutectogel costituiscono un buon sistema per il rilascio controllato di etosuccimide, che avviene attraverso un meccanismo di diffusione quasi-Fickiano.

Parole chiave: Eutectogel, Etosuccimide, Drug delivery, Diffusione, HR-MAS NMR

Content

Acknowledgements

First of all, I would like to thank my advisor Prof. Franca Castiglione and my co-advisor Valeria Vanoli, for the opportunity to work on this project, trusting me and guiding me during this work.

To my family, who have always been by my side and never stopped believing in me. I will never thank you enough for being with me during the most challenging times. Even though we have been separated for the last few years, I have never stopped feeling your presence with me.

Finally, I would like to thank all people who I have met in my journey abroad, for keeping up with my life and motivating me to finish my studies and conclude my master thesis.

1 Materials

1.1. Deep Eutectic Solvents

Deep eutectic solvents (DESs) are a fairly new concept, which first appeared in scientific literature in 2003. Although deep eutectic solvents have been intensively explored, particularly in the past decade, the formation principle and features of deep eutectic solvents are still poorly understood. According to Andrew Abbott [1], who first described DES systems, they are a mixture of certain hydrogen bond donors (HBDs) and acceptors (HBAs) [2, 3]. DES are cheap, easy to prepare and non-toxic as they can be obtained from compounds of natural origin. The characterization of selected compounds is based on their physicochemical properties, and their molar ratio [4]. We can classify DESs as a class of Ionic Liquids (ILs) due to the common characteristic as high thermal stability, low volatility, low vapor pressures and tuneable polarity [5]. Their properties such as low preparation costs, environmentally friendly, wide polarity range, low vapor pressure and volatility, non-inflammability, thermal and chemical stability, biodegradability, and low toxicity [6] make DESs a promising approach in the field of drug delivery science and a good choice for large-scale applications for the synthesis of functional materials [7].

The idea behind their operation is the mutual reduction of the melting point by the components of the mixture, consequently the DES melting point is lower than the melting point of their individual components. The most known example of DES is a mixture of choline chloride and urea. Under normal conditions, the two components are solids with a very high melting points (choline chloride = 302 ℃ and urea = 133 ℃), but when mixed at the right proportions they melt at 12 ℃ [1].

There are various possible techniques for producing deep eutectic solvents, such as stirring (either with or without heating), freezing and vacuum evaporation methods. The choice of the methodology relies on personal preference, available equipment, and ability to minimize water content [5].

1.1.1. The phase diagram of eutectic solvents

To better understand the meaning and characteristics of Deep Eutectic Solvents, it is important to analyse their phase behaviour, mainly focusing on the concept of eutectic point. Frederick Gutherie, in 1884 used the term eutectic, originally from the Greek, which means "easy (or lowest than an individual) liquefaction" [8, 9].

Deep eutectic solvents are mixtures of two or more pure compounds. This system can be visualized using a solid-liquid phase diagram (Figure 1) that shows the melting point as a function of the mixture's composition [10]. According to Martins et al. [11] the term "deep eutectic solvent" should only refer to mixtures with a melting point lower than the ideal eutectic temperature; otherwise, deep eutectic solvents would be indistinguishable from other eutectic mixtures. Furthermore, a deep eutectic solvent must be liquid at operating temperature, even if this demands a non-eutectic composition. To determine the ideal solubility curve, it is necessary to have a phase diagram and knowledge of the melting properties of pure compounds. The eutectic point represents the composition and minimum melting point where the melting curves of both compounds meet in a binary mixture of two compounds, A and B. Most deep eutectic solvents have freezing points ranging from – 69 to 149 ℃, but all have a freezing point lower that 150 ℃, which can influence the freezing point of the mixture. The freezing point of the mixture can be affected by the hydrogen bond donor, the nature of the organic salt and its anion, and the molar ratio of the hydrogen bond donor to the organic salt [12, 13].
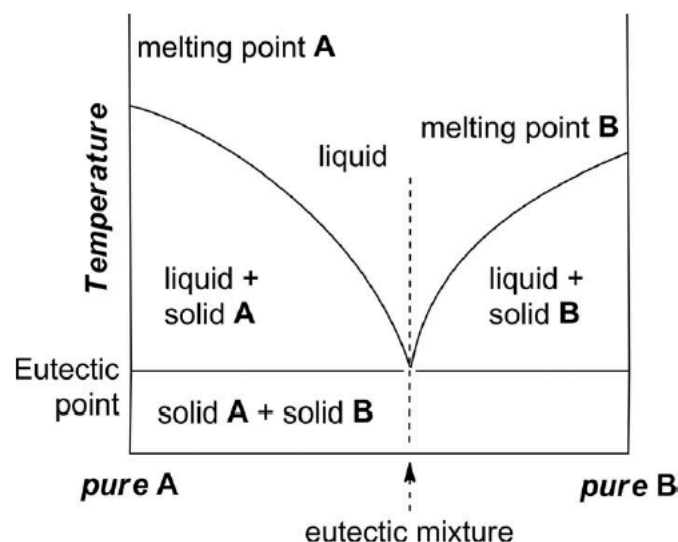

Figure 1: Phase diagram for two compounds, A and B, eutectic formation [8, 14].

1.1.2. Properties of Deep Eutectic Solvents

There are several types of DESs, which are summarized in table 1.1 according to their composition [15].

Besides the already mentioned conventional DESs, there are also natural deep eutectic solvents (NADES) and therapeutic deep eutectic solvents (THEDES). NADES is a new class of DESs which are based on complexations of primary metabolites or bio-renewable ingredients such as amino acids, sugar alcohols, sugars, and organic acids [16]. The ingredients that contribute to the formation of NADES exhibit incomprehensible natural phenomena such as the solubility and biosynthesis of semipolar components that are neither soluble in water nor in the lipid phase. Based on research, NADES are considered as a non-toxic and biodegradable and with the time they can become an alternative to ILs and DESs [3]. THEDES – therapeutic deep eutectic solvents - have been defined as a bioactive eutectic system containing an active pharmaceutical ingredient (API) as one of the DES components [17, 18]. One of the limits of application of THEDES can be the lack of evidence in regarding with safety, toxicity, and some other pharmaceutical issues such as pharmacokinetic behaviour [6]. But generally, based on scientific formulating THEDES delivery systems would preserve THEDES bioavailability, improve their stability and ultimately promote controlled release to achieve therapeutic effect [19, 20].

Table 1.1: Classification of DESs [21].

Type	Composition: HBD and HBA	Example
I	Organic salt + Metal salt	Choline chloride + $ZnCl_2$
II	Organic salt + Hydrated metal salt	Choline chloride + $CaCl_2.6H_2O$
III	Organic salt + Hydrogen-bond donor	Choline chloride + Urea
IV	Metal chloride + Hydrogen-bond donor	$ZnCl_2$ + Urea
V	Non-ionic hydrogen-bond acceptor + Non-ionic hydrogen-bond donor	Citric acid + glucose

The properties of DESs are based on the molecular ratio of the components, that are described below:

- *Density* is one of the most important properties of DESs, because can provide information about intermolecular interactions in a DES. DESs have densities that are higher than the density of water and the HBD and the density of DES decreases linearly as temperature rises. Regarding to analysed literature the

density of DESs depends on temperature, organic salt/HBD molar ratio, structures of HBD and HBA, and choice of hydrogen bonding donor [15].

- *Viscosity* describes the resistance of a fluid in response to a deformation at a given shear rate. The viscosity of an eutectic mixture is also affected by the nature of its components, the HBA/HBD molar ratio, the temperature, and the water content. Usually, DESs exhibit 100-1000 times higher viscosities at room temperature than water and common organic solvents due to the formation of an extensive hydrogen-bonding network between HBD and HBA [15]. High viscosity can cause problems for applications for DESs in pharmaceutical operations such as handling, mixing, and filling [3].

- *Ionic conductivity*, DESs exhibit lower properties of conductivity than other ionic liquids and molecular solvents at room temperature [22]. The viscosity decreases with increasing the temperature, so the ionic conductivity of DESs increases with temperature. Ionic conductivity is affected by the hydrogen bond acceptor/hydrogen bond donor molar ratio, the nature of both the organic salt and the hydrogen bond donor as well as the salt's anion [12].

- *Surface tension* is a measure of the energy necessary to increase the surface area of a material and relates to the tendency of the material to have the smallest possible surface area. Regarding studies for DES's surface tension are limited in comparison with other physicochemical properties. Surface tension plays important role as a property which is highly dependent on the intensity of the intermolecular forces taking place between the hydrogen bond donor and corresponding salt [12].

- *Polarity* of deep eutectic solvents hasn't been properly studied although it is a key property in the matter of solvation capability of solvents [23]. DESs have high polarity, which can be evaluated using the E_T scale (electronic transition energy of a probe dye in a solvent).

- *Toxicity*, according to the study of Chabib et al. [15], the type of individual components, interaction with living organisms, pH of the DESs, synergistic effect, and molar ration affect the toxicity profile of DESs. Most components of DESs are rather non-toxic, biodegradable, and pharmaceutically acceptable, but the toxicity of different DESs varies depending on the structure of the components. Furthermore, some DESs are far more toxic than their precursors.

It is important to determine the toxicity, biocompatibility, and biodegradability profiles before applying it to pharmaceutical applications [3].

- *Hygroscopicity* is the tendency of a material to take up water vapor from the surrounding air. DESs, due to their hydrophilic nature and hydrogen bonding network, exhibit rather high hygroscopicity and the absorption of moisture from air, additionally the presence of water can highly affect the structure and physicochemical properties of DESs [3].

1.1.3. Deep Eutectic Solvents as drug delivery systems

Nowadays drug delivery systems are a very important branch in the medical sector. There are many strategies that enable drug delivery, involving both modifications of conventional methods and design of new solutions [24]. Polymers play an important role thanks to their ability of encapsulating therapeutic agents and releasing them in constant doses over long periods. Scientific research shows that DESs can be used in a wide range application as they are efficient as biopolymer modifiers, solubilizing vehicles, and drug delivery systems for controlled release applications [25]. For example, Pereira et al. [26] focused on the study of the novel Limonene-based THEDES compounds due to its well-known and remarkable anticancer properties. Limonene (LIM) has been combined with a variety of compounds, including fatty acids, menthol, and non-steroidal anti-inflammatory drugs (Ibuprofen), prepared in various molar ratio, equimolar or unbalanced ratios. In-depth analysis and research have shown that Ibuprofen:Limonene (1:4) has the best properties. Indeed, this THEDES contains protective and anti-inflammatory properties of ibuprofen allied with the anti-cancer properties of LIM and shows the efficient proliferation of human colon cancer cells without affecting the viability of healthy cells. Limonene-ibuprofen DES not only kept the therapeutic effect but also increased the solubility of the two components and reduced the side effect of limonene on the viability of normal cell lines. The use of this type of THEDES will reduce the cellular cytotoxicity, which further demonstrates the potential of this system as a drug delivery system in anti-cancer therapies. Another eye-catching example might be the use of API-DES in transdermal drug delivery systems with the combination of rotigotine using in the treatment of Parkinson's disease [4]. The encapsulation of the drug in an API-DES allowed to improve not only the skin permeability of the drug, but also the drug-polymer miscibility, with a consequent improvement of the transdermal drug delivery process.

DESs-based systems for controlled drug delivery scan provide satisfactory results in many medical fields such as oral drug delivery, buccal drug delivery, nasal drug delivery and much more, and they are many future concepts to discover.

1.2. Materials

1.2.1. Menthol

Menthol, also known with the name mint camphor, is a white, crystalline phenolic compound very soluble in alcohol, chloroform, ether, and hexane, can be isolated from essential oils of corn mint and peppermint [27]. The most characteristic property of menthol is the minty smell. It exhibits properties such as effectiveness as permeation enhancer together with well-known anti-inflammatory and antimicrobial properties. Menthol can be extracted from *Mentha* species, and it has been already used for THEDES preparation in combination with a wide range of compounds including ibuprofen, lidocaine, fluconazole, and captopril [28]. According to the European Commission and the Food and Drug Administration (FDA) it is classified as "generally recognized as safe" (GRAS), but the mucous membranes of the gastrointestinal tract can experience burning sensation after inhalation ≥ 200 mg and ingestion ≥ 8000 mg, which in some cases might become serious.
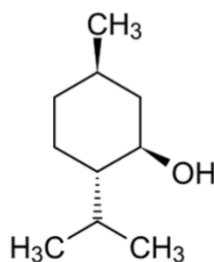
Figure 2: The chemical structure of menthol [29].

1.2.2. Thymol

Thymol is a natural monoterpenoid phenol. At toom temperature it is a crystalline and colourless compound with low water solubility and a characteristic flavour and smell of thyme [30, 31]. Thymol is used for many medical purposes such as treating ailments affecting the respiratory and digestive systems (antitussive, expectorant, stomachic, digestive, carminative, and antispasmodic), activity against oral diseases such as caries, antioxidant, anti-inflammatory, antifungal, and antimicrobial activities. The European Commission and the Food and Drug Administration (FDA) found it as "generally recognized as safe" (GRAS), but prolonged exposure and intake of amounts higher than recommended may occur as toxic [32].
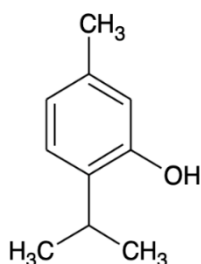
Figure 3: The chemical structure of thymol [33].

1.2.3. Ethosuximide

Ethosuximide (2-Ethyl-2-methylsuccinimide) is an antiepileptic drug, and it is commonly considered as a first-line treatment for absence seizures due to its well-established efficacy in the field [34]. It has the potential to treat a number of neuropsychiatric illnesses, including Parkinson's disease, and has been found to have neuroprotective, antinociceptive, and life-extending benefits. Although typically well tolerated, the use of ethosuximide in various seizure types and epileptic syndromes in constrained by its limited range of therapeutic activity [35].
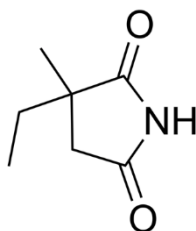

Figure 4: The chemical structure of ethosuximide [36].

1.3. Eutectogels

Currently, due to the problems related to poor temperature resistance, low conductivity, bioincompatibility and high costs, traditional gels using water, organic solvents, ionic liquids, and continuous phases face several contraindications for wide applications. Gels are well-known soft colloidal materials characterized by a "solid-like" three-dimensional network. Cross-linked and entangled polymers or small molecules (low molecular weight gelators, LMWGs) that self-assemble into a nanoscale network as a result of intermolecular non-covalent interaction are most frequently responsible for creating the solid-like network in gels. Ionogels, gels based on ILs have undergone tremendous development, whereas gels based on deep eutectic solvents (eutectogels) have attracted far less attention. Eutectogels have promising

properties, the prospect of which will allow applications in medicine, energy, electronics, and environmental science compared to temperature-resistance hydrogels and expensive ionogels as flexible ionic conductors. They exhibit inherent high electrical conductivity, low volatility and hight thermal stability, and low DESs costs. Because of the use of physically interacting polymer networks, they have the advantage of dynamic recyclability and biosafety, making them an alternative to chemically cross-linked gels. They do not have adequate stability and mechanical strength due to weak non-covalent interactions. Different methodologies can be used to improve the mechanical-physical properties of the hydrogels, but they cannot be applied to eutectogels due to internal differences in the physical and chemical properties of DES components and water. Developing strong and physically resistant eutectogels remains a significant challenge [37, 38].

So far, scientific research on eutectogels is very limited and there are not a lot of scientific publications with adequate results, however DESs eutectogels can be shortly divided into three types:

   I.   Polymer gels in which DESs only act as solvents (Eutectogels-S)
  II.   Polymer gels in which DESs act as a solvents and polymerized monomers (Eutectogels-P)
III.   Supramolecular gels in which DESs act as solvents (Supermolecular Eutectogels) [39]

In 2018, the concept of supramolecular gels (SEGs) was presented for the first time by two independent research studies. The first study, by Marullo et al., used choline chloride-phenylacetic acid (1:2) DES and L-amino acids: isoleucine and tryptophan as chelating agents. The supramolecular gel was formed through the route of gel-sol transition. Its high mechanical strength and environmental friendliness have been proven, making it a promising material for applications that require high mechanical properties. The second study (Florindo et al.) used a supramolecular DES gel containing metal ions with application of hydrophobic DES, combining a dodecanoate sodium salt as an HBA and carboxylic acid as an HBD. A small addition of water as an antisolvent of DES resulted in the precipitation of a supramolecular gel. This discovery has promising potential for biomedical applications. One of the latest discoveries is the use of 1,3:2,4-dibenzylidene-D-sorbitol (DBS) as a gelling agent. It was used by Ruiz-Olles et al. [38] who added it to DES formed with choline chloride and alcohol/urea, as a result of intermolecular non-covalent interactions a supramolecular DES gel was formed (Figure 5). This study showed similar electrical conductivity for both eutectogels and liquid DESs, contributing to great potential in the fields of energy and catalysis [39].
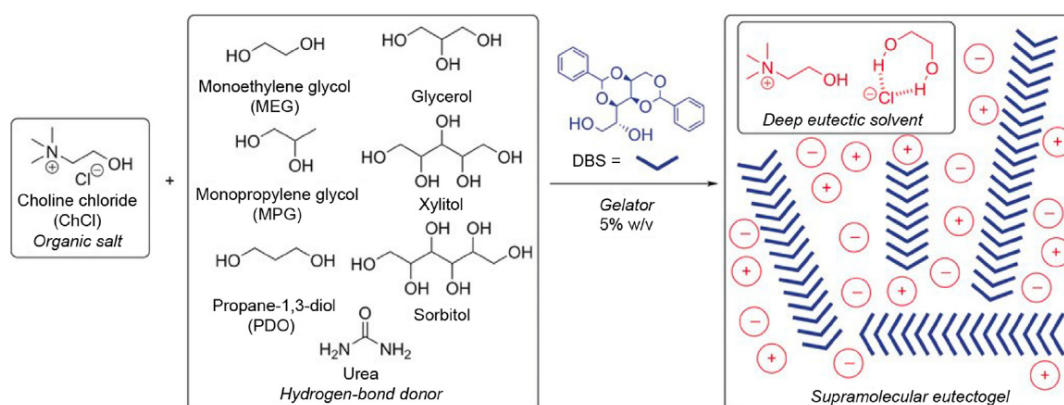
Figure 5: Formation of supramolecular eutectogels by mixing organic salt and hydrogen bond donor with 1,3:2,4-dibenzylidene-d-sorbitol (DBS) [39].

1.3.1. 1,3:2,4-Dibenzylidene-D-sorbitol (DBS)

Dibenzylidene-D-sorbitol is a well know low-molecular-weight chiral oil gelling agent, it is a chemical derivative of the natural sugar alcohol D-glucitol [40]. It is a highly versatile self-assembling system which has remarkably been known for well-over 100 years and found in many applications [41]. Little amounts of DBS easily dissolve in a variety of organic solvents at high temperatures. DBS molecules can strongly interact in the presence of an organic liquid and, under the correct circumstances, self-organize to form a molecular network thanks to their butterfly shape and propensity to create intermolecular hydrogen bonds between the terminal hydroxyl group and the acetal oxygens [40]. In this research work DBS has been shown to be an effective gelling agent of glycols such as 1,2-ethylene glycol, in the presence of polar additives such as water [38] which can form thermally reversible gels.
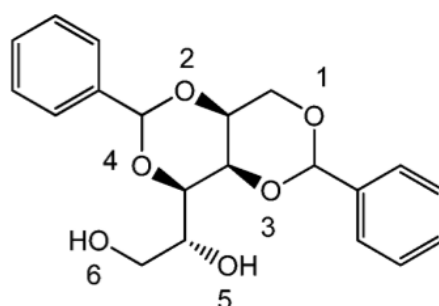

Figure 6: The chemical structure of 1,3:2,4-Dibenzylidene-D-sorbitol (DBS) [41].

2   Methods

2.1. Nuclear Magnetic Resonance (NMR) Spectroscopy

Nuclear Magnetic Resonance Spectroscopy is a technique commonly used in the analysis of the structure, properties, and interactions of chemical compounds. The use of NMR spectroscopy is possible in the study of liquid samples (pure substances, their solutions, and other mixtures), solid and semi-solid (gels) samples. The dimensions of the characterizable compounds range from small inorganic and organic molecules to huge molecules of natural and synthetic polymers. The use in pharmacy and structural biology is not limited to determining the structure of the tested particles but also to describe their internal dynamic, as well as mutual interactions. NMR spectroscopy uses electromagnetic radiation with frequencies in the radio range (60 – 900 MHz, although continuous work on improving spectrometers will lead to the introduction of devices measuring at higher and higher frequencies), which compared to the one used in other spectroscopic methods, carries a small amount of energy. NMR spectroscopy is, in fact, an absorption spectroscopy and results of experiments can describe the energy absorbed by the sample. One-dimensional spectra are graphs with the amount of energy quanta of electromagnetic radiation absorbed by the sample as a function of the frequency of this radiation [42, 43].

2.1.1. Basic theory

Quantum mechanical subatomic particles (protons, neutrons, and electrons) possess a property known as spin. In particular, nuclei with an odd number of protons and/or neutrons possess a spin, characterized by a nuclear spin quantum number, m_s, which is different from zero and therefore they are "NMR-active". Several nuclei that are the basis of organic compounds are "NMR-active" and can be observed, they include the isotope of hydrogen ^{1}H, the isotope of carbon ^{13}C, the isotope of nitrogen ^{14}N, ^{19}F and ^{31}P. The commonly known carbon isotopes ^{12}C and oxygen isotope ^{16}O have $m_s=0$, which makes it impossible to observe them using NMR, conversely ^{1}H and ^{13}C nuclei are the most used in NMR research. Because the ^{1}H atom's nucleus is a single proton, ^{1}H NMR is also known as proton NMR [43, 44].

Nuclear spins are random in their directions in the absence of an externally applied magnetic field (B_0), while nuclei align either with or against the external magnetic field when it is present. Each proton can take one of two possible orientations with respect to the external magnetic field. α and β states are two orientations that correspond to two spin states (1/2 and -1/2). The α spin state is in the direction of the external magnetic field B_0, and the β spin state is in the opposite direction to B_0 (Figure 7).
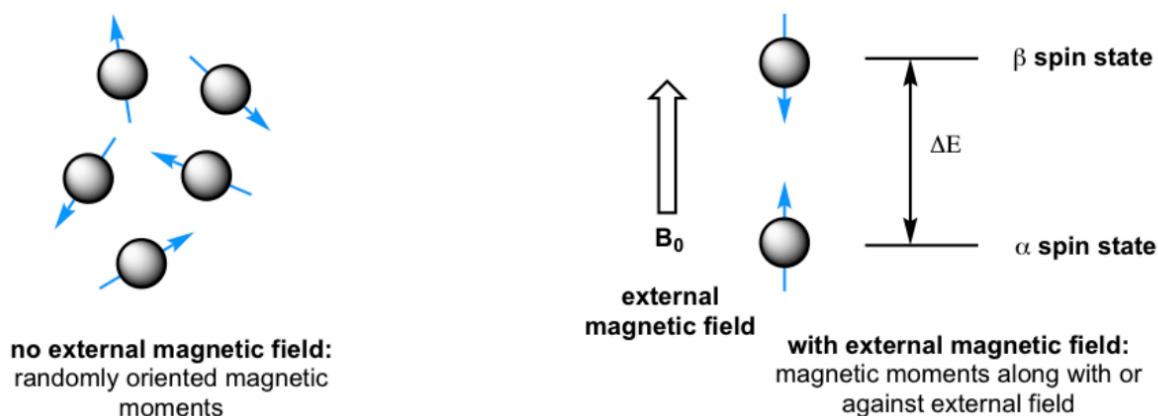
Figure 7: Proton magnetic moment orientations.

In an external magnetic field, the majority of spins are found in the lower energy α spin state, according to the Boltzmann distribution:

$$\frac{N_\alpha}{N_\beta} = e^{\Delta E/k_B T} \qquad (2.1)$$

where $N\alpha,\beta$ is the number of nuclei in the two states, k_B is the Boltzmann constant and T is the temperature. NMR technique takes advantage of the population difference between the two spin states, which increases with the strength of the applied magnetic field B_0. Energy is needed to excite a proton from an α state, which has lower energy, to a β state, which has more energy.

An alternative approach to describe NMR phenomenon is based on the classical mechanics. The spinning nucleus (Figure 8) possesses angular momentum (I), and charge, and the motion of this charge gives rise to an associated magnetic momentum (μ_{spin}) such that:

$$\mu_{spin} = \gamma \cdot I \qquad (2.2)$$

where the term γ is the gyromagnetic ratio, which is constant for any given nuclide (for example $\gamma = 2.675 \cdot 10^8$ T^{-1}s^{-1} for ^{1}H). Both angular momentum and the magnetic quantum moment are vector quantities, that is, they have both magnitude and direction. The quantized z-component of the angular momentum I is:

$$I_z = \hbar m_s \qquad (2.3)$$

where $\hbar$ is the ratio between Planck's constant and 2π and $m_s = \pm\frac{1}{2}$ for ^{1}H.

Consequently, the magnetic momentum μ_{spin} is quantized and its z-component can assume different orientations, due to m_s values:
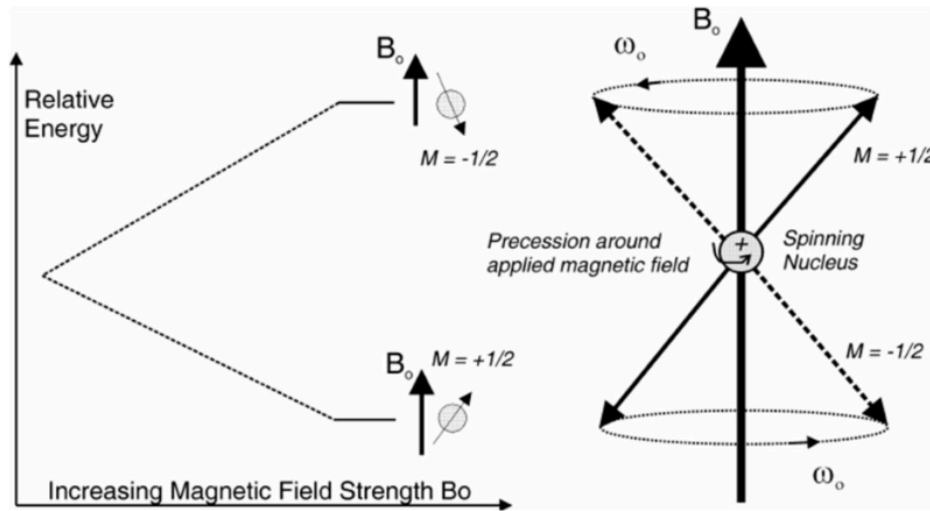
$$\mu_z = \gamma I_z = \gamma \hbar m_s \qquad (2.4)$$

Figure 8: Change in energy difference between two spin state and precession of a spin with angular frequency ω_0.

The effect of a static magnetic field B_0 is to impose a torque over μ which starts processing giving rise to the Larmor precession (Figure 8). The rate of the precession as defined by the angular velocity $\omega_0 = -\gamma B_0$ in rad/s or the Larmor frequency ν_0 in Hz, defined as:

$$\nu_0 = -\frac{\gamma B_0}{2\pi} \qquad (2.5)$$

The potential energy E of the nucleus in one of the two directions can be expressed as:

$$E = -m_s \gamma B_0 \hbar \qquad (2.6)$$

with $m_s = +1/2$, for the lower energy state:

$$E_{+1/2} = -\gamma B_0 \frac{\hbar}{2} \qquad (2.7)$$

and $m_s = -1/2$, for the higher energy state:

$$E_{-1/2} = \gamma B_0 \frac{\hbar}{2} \qquad (2.8)$$

The difference in energy between levels (the transition energy):

$$\Delta E = \gamma \hbar B_0 \qquad (2.9)$$

An increase of magnetic field B_0 means that ΔE is also increased. Additionally, if a nucleus has a comparatively high magnetogyric ratio, then ΔE will be also high.

NMR phenomenon occurs when the nucleus changes its spin state from a lower energy state (α spin state) to a higher energy state (β spin state), driven by the absorption of a quantum of energy [42, 43, 44, 45]. This energy, in radio-frequency range, must match that of the Larmor precession:

$$E = h\nu_0 = \gamma\hbar B_0 \qquad\qquad (2.10)$$

This is the "resonance" condition.

In a macroscopic sample, all the spins will be processing randomly about Bo at their Larmor frequency. The vector sum of all the magnetic moments gives a single vector pointing in the direction of the applied magnetic field called the macroscopic magnetization, M_0.

2.1.2. Fourier Transformation in NMR analysis and relaxation phenomena

The signal emitted by excited atoms, called FID (free induction decay), is oscillating with a frequency equal to the Larmor frequency of the analysed nuclei, and over time it decreases exponentially in proportion to the progress of the relaxation phenomena. The FID is recorded by the spectrometer and a Fourier transform is then applied. The Fourier transform allows to relate a time-dependent signal *S(t)* to a frequency dependent one and is the most important of the processing operations that are normally performed on raw NMR data. The resulting NMR spectrum is a graph plotting the intensity of the peak's *vs* the frequencies [43].
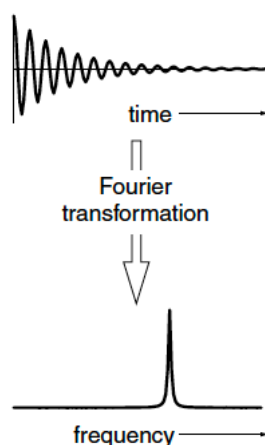

Figure 9: Fourier transformation as the mathematical process.

In NMR, it is crucial to consider where the energy moves and, in particular, how quickly it "gets there". The nuclei in the excited state must be able to relax and return to the ground state because the NMR process is an absorption process. The relaxation time scale and mechanisms, due to the transfer of thermal energy from the excited state to the environment, are fundamental to the NMR experiment [45]. Relaxation

combines 2 different mechanisms that act together, with characteristic times T_1 and T_2 respectively:

- Longitudinal or spin-lattice relaxation

$$M_z = M_0[1 - exp(-t/T_1)] \qquad (2.11)$$

- Transversal or spin-spin relaxation

$$M_y = M_0 exp(-t/T_2) \qquad (2.12)$$

2.1.3. Chemical shift

NMR spectroscopy in chemistry is based on the ability to distinguish a specific nucleus due to the molecular environment, i.e. the arrangement of electrons in a molecule's chemical bonds affects the resonance frequency of a single nucleus. Because the protons in the analyte have distinct chemical surrounding, different peaks are observed in the proton spectrum. A chemical shift of the resonance frequency, or just a chemical shift, is the term used to describe this phenomenon. According to Lenz's law, this means that the static magnetic field B_0 causes the electron cloud to circle the nucleus, and a magnetic moment opposite to B_0 develops as a result.

Consequently, the local field at the nucleus is smaller than B_0, because of the shielding of the nucleus itself, and the local nuclear field B_{local} is:

$$B_{local} = B_0(1 - \sigma) \qquad (2.13)$$

where σ is the shielding or screening constant of the nucleus. The resonance requirement is met at field strengths that are different from those predicted theoretically because of the shielding constant, which is proportional to the electron density of the electron core.

- Protons that have been shielded have reduced chemical shift (δ) values and a lower resonance frequency.
- Protons that have been deshielded have a higher resonance frequency and larger chemical shift (δ) values.

The position of the resonant frequency is related to a reference compound tetramethylsilane (TMS) for proton NMR. The introduction of a dimensionless quantity, with the following definition, made it possible for the values of chemical shifts to be independent of the strength of the field:

$$\delta = \frac{v_{substance} - v_{reference}}{v_0} 10^6 \qquad (2.14)$$

where v_0 is the working frequency of the spectrometer.

In this way, NMR data are given in terms of a chemical shift (δ) over a scale of 0-10 the parts per million ppm - δ scale (Figure 10). By convention, the right-hand side of an NMR spectrum with smaller chemical shift values is called upfield, and the left-hand direction is called downfield (Figure 10).
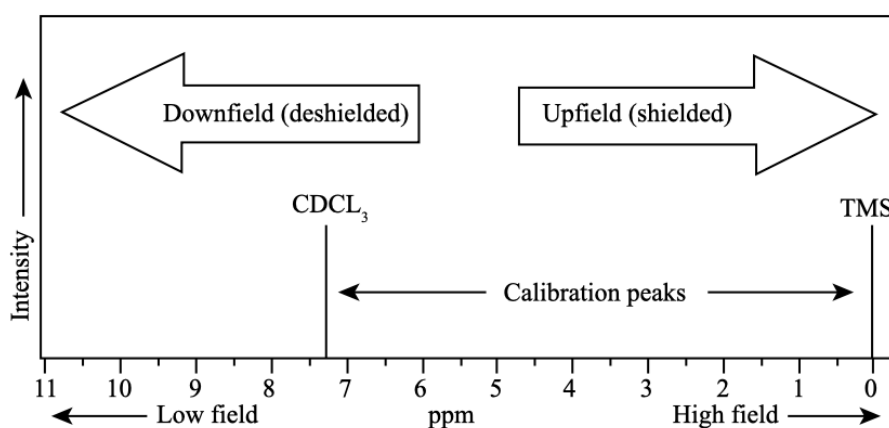

Figure 10: The chemical shift scale in H NMR spectra.

Chemical shift information is significant because it provides essential hints regarding the molecular structure. The chemical shift of some functional groups is shown in Figure 11:
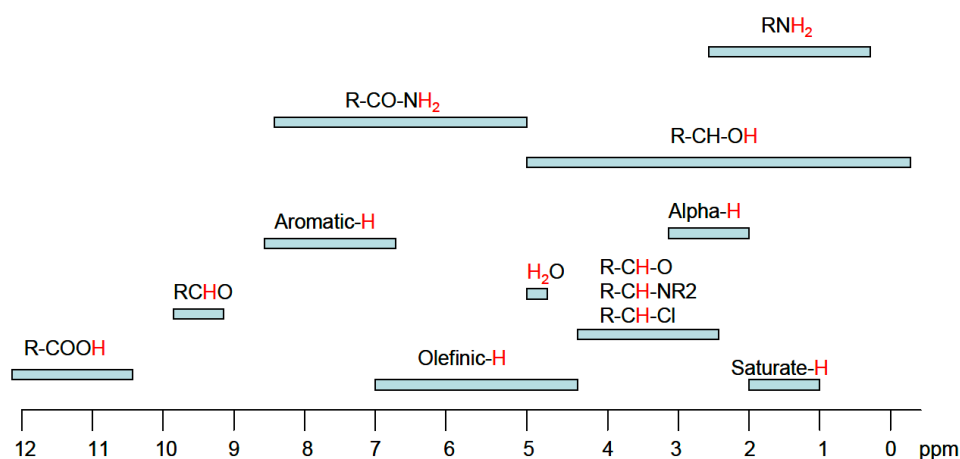

Figure 11: Table for various cases of the chemical shift.

2.1.4. 2D NMR-diffusion

1D NMR spectra are graphs of the signal's intensity versus frequency. In 2D spectroscopy, on the other hand, the intensity of the signal is described as a function

of two frequencies. The 2D graph is often done by plotting signal peaks by contour lines at a location specified by two frequency coordinates.

In 2D experiments, the signal is recorded as a function of two-time intervals t1 and t2, consequently the data is Fourier transformed twice so as to be a function of two frequencies f1 and f2. A two-dimensional matrix is obtained characterized by diagonal peaks and cross peaks. The peaks in diagonal are centered around the same coordinates f1 and f2 and represent the corresponding one-dimensional spectrum; cross peaks, however, are cantered around different coordinates of f1 and f2 and represent the magnetization transfer due to spin-spin coupling (*J*), or to more complex dipole interactions.

NMR spectroscopy allows measurement of molecular self-diffusion coefficient, D, by performing a pseudo-2D experiment. The diffusion rate is often related to the hydrodynamic properties and size of the molecule indicative of its aggregation state.

In a typical diffusion-NMR experiment, pulse field gradients (PFG) are used to encode/decode the physical location of a particle in solution and thus characterise its diffusion motion. During the measurement of diffusion, molecules undergo translational motion between two gradient pulses: the first pulse is to dephase the magnetization and the second pulse is to refocus after a time delay (Δ). The observed signal will be reduced ($I < I_0$) because the refocusing gradient will not properly restore the transverse magnetization to its initial phase. The greater the displacement of the spins during Δ due to diffusion, the more reduced the observed signal intensity. This sequence is repeated many times by progressively increasing the intensity of the gradient but keeping its duration constant. A pseudo-2D experiment is obtained in which the intensity of the signal is a function of the strength of the gradient. The signal decay is fitted by the Stejskal-Tanner equation:

$$I = I_0 exp\left(-(\gamma\delta G)^2 D\left(\Delta - \frac{\delta}{3}\right)\right) \qquad (2.15)$$

where G is the strength of the gradient, δ the duration of the gradient, D the diffusion coefficient and Δ the diffusion time [46].

2.1.5. High-Resolution Magic Angle Spinning (HR-MAS) NMR Spectroscopy

The innovative High-Resolution Magic Angle Spinning (HR-MAS) method was developed in 1996 in order to enable NMR applications directly on heterogeneous semi-solid and gel-like substrates [47]. Since it allows to get spectra on complete, unaltered semi-solid materials with a resolution comparable to that of liquid-state spectroscopy, HR-MAS is a combination of solid- and liquid-state NMR techniques. In fact, semi-solid samples still have enough molecular mobility to effectively minimize the variables that influence solid-state NMR results. HR-MAS probes combine magic

angle spinning found in solid-state MAS probes with lower power radio frequency (RF) handling, a lock channel, and pulsed field gradients that are typical of solution-state NMR. The rotor, after being inserted into the HR-MAS probe is spun at an angle θ=54.74° (referred to as the "magic angle") with respect to the external magnetic field (B_0) at a moderate rate (v_R) (Figure 12). [48, 49]. The magnetic susceptibility, chemical shift anisotropy (CSA), and dipolar interactions that cause spectral line broadening, can all be suppressed using the MAS system. The Hamiltonian that describes these significant spectral-broadening interactions has an angular dependence of:

$$\frac{3cos^2\theta-1}{2}$$ (2.16)

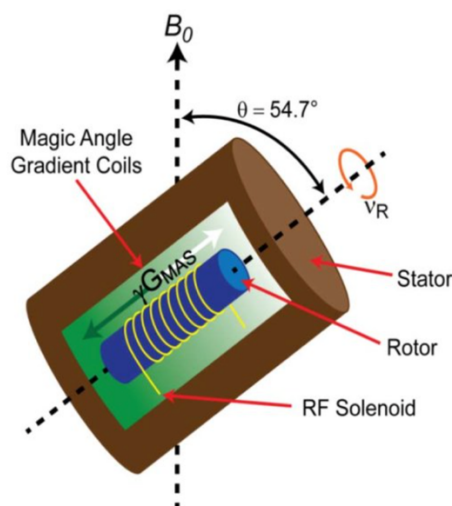where is θ the angle between the static magnetic field and the inter nuclear vector that drives the interactions.

Figure 12: Scheme of a HR-MAS stator with a magic angle gradient along the rotor spinning axis.

This technique produces ^{1}H NMR spectra with great resolution that are remarkably similar to those found in solution NMR (Figure 13). MAS speeds between 1 and 2 kHz can increase resolution for liquids adsorbed in or on materials, while MAS speeds between 4 and 12 kHz may be required for plasticized or swollen materials to provide the required resolution. In addition, care must be taken to ensure that residual rotating sidebands (caused by insufficient averaging) fall outside the target spectral region [50, 51, 52]. The same pulse sequences that are used for traditional solution NMR investigations can also be used for multidimensional NMR experiments.
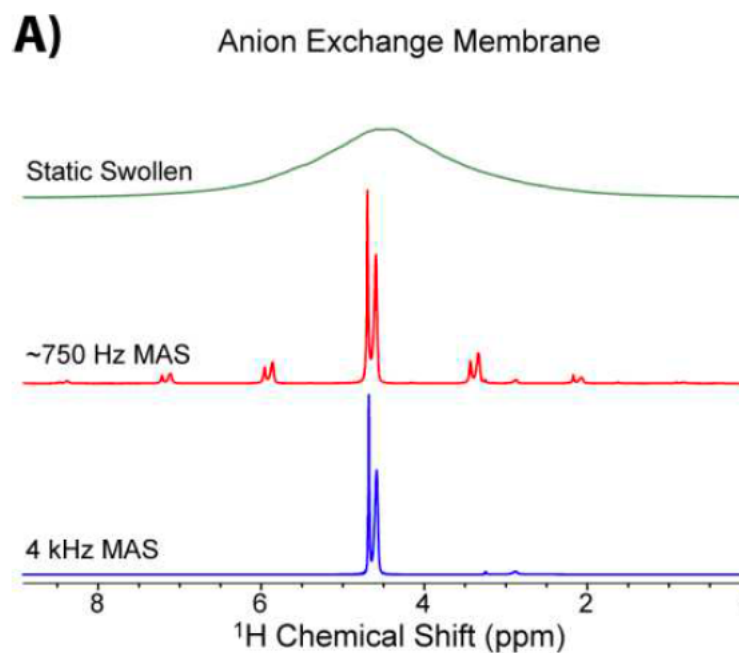
Figure 13: [1]HR-MAS technique with peaks resolution, swollen polymer system.

Liquids or substances that resemble liquids are prevalent in HR-MAS samples. These samples must be handled carefully to avoid dehydration which can happen in a typical rotor with just a rotor lid. Figure 14 shows some of the inserts that are commercially available for packing HR-MAS samples.
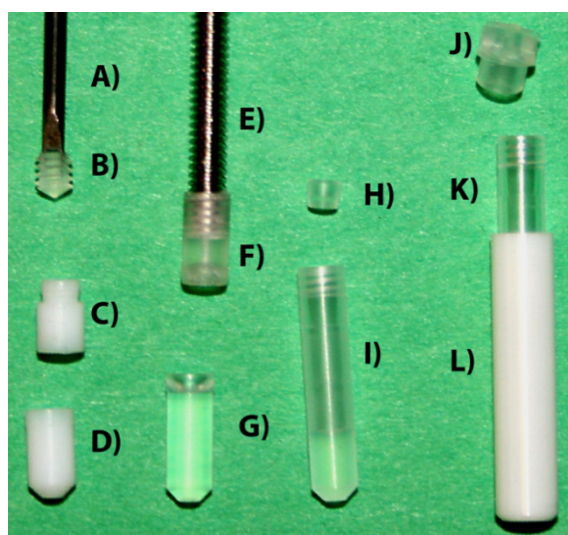

Figure 14: The tools and inserts used for HR-MAS NMR.

2.2. Infrared (IR) spectroscopy

2.2.1. Basic theory

Infrared spectroscopy (IR) is one of the most commonly used spectroscopic technique in organic and inorganic chemistry. It consists in measuring the absorption of infrared radiation of various wavelengths by the tested sample located in the path of the beam. IR spectroscopy enables examinations of solid substances (crystals, powders, gels), liquids and gases.

Due to the principle of operation, IR spectrometers can be divided into dispersion spectrometers and FTIR spectrometers, i.e., Fourier transform IR spectrometers. Almost all spectrometers in use today are FTIR spectrometers. In dispersion spectrometers, the sample is irradiated with almost monochromatic beams of radiation. In the case of an FTIR spectrometer, the sample is exposed to radiation from the entire range simultaneously, and less energy is lost between the source and the detector. Thanks to this, the recording of spectra using the FTIR spectrometer is much faster, and the measurement sensitivity is likewise higher.

The region of the electromagnetic spectrum with a wavenumber from about 14000 to 200 cm^{-1} between the visible and microwave regions is called infrared (IR). In determining the structure of organic compounds, the range of 4000-400 cm^{-1} (the basic infrared region) has the greatest application, with far-infrared (below 400 cm^{-1}) and near-infrared (above 4000 cm^{-1}) adjacent to it. Due to the type of oscillatory vibrations in which the particle is set, there are several types: symmetrical and asymmetrical stretching and bending.

FTIR spectroscopy makes it possible to determine the characteristic vibrations for the groups present in the compound. Because the FTIR spectrum is a spectrum characteristic for a given substance, infrared spectrophotometric analysis is most often used for qualitative research. In addition to distinguishing pure substances, the FTIR analysis can also test the presence of additional substances as well as their interactions with individual groups of the original compound [53, 54].

2.3. Scanning Electron Microscopy (SEM)

2.3.1. Basic theory

Scanning electron microscopy (SEM) is a measurement technique that provides information about the morphology and topography of a surface by scattering electrons. Thanks to electrons, the resolution obtained is higher than that obtained with optical microscopes.

It consists of an electron gun used to generate high energy electrons which are then focused on the sample; a column in which the electron beam is accelerated and focused; sample chamber, where electrons of the beam interact with the sample, a set of detectors receiving various signals emitted by the sample and signal-to-image processing system. SEM images the sample by scanning it with a highly focused beam of electrons. By striking individual atoms in the test sample, electrons are then detected, and information on surface details as well as internal structure can be extracted.

To create the image secondary signals, generated because of the interaction of the primary electron beam with the sample, are used as listed below:

- Secondary electrons (SE) – they are formed in a large amount as a result of inelastic collisions of electrons bombarding the sample with electrons of outer shells. Some of them thus obtain sufficient energy to overcome the potentials barrier and "exit" from the material; the emission of secondary electrons depends on the accelerating voltage. An important feature of secondary electrons is the dependence of their emission on the angle of incidence of primary electrons, which is used in surface topology studies.
- Backscattered electrons (BSE) – they are formed as a result of elastic collisions; their emission is not dependent on the accelerating voltage. They are characterized by low intensity, for surface imaging the dependence of their emission on the atomic number is used, thanks to which they are used to distinguish areas of different chemical composition.
- X-rays – they are emitted as a result of the electron being knocked out of the inner shell and the electron jumping from a higher energy level to a free spot in the inner shell, accompanied by the release of energy. The radiated quantum of radiation can cause the emission of Auger electrons used in the study of surfaces layers; the energy and wavelength of the emitted X-ray radiation are characteristic for individual elements, thanks to which they are used to analyse the chemical composition in micro-areas.

The scanning electron microscope has a large depth of field, so it produces an image that is a good representation of a three-dimensional sample. The combination of higher magnification, greater depth of field, greater resolution, compositional and crystallographic information make SEM one of the most popular techniques [55].

3   Drug release profile

3.1.   Basic theory

Drug delivery is a rapidly growing field with the aim to improve the effectiveness of drug therapy. Although it is still a quite new scientific discipline, over the past few decades significant medical advances have been made to achieve a relevant contribution [56]. The highly disciplinary nature of the field makes the engineers a unique role in the development of new strategies for drug delivery with many scientific results and analysis focused on the drug delivery [57]. Traditional drug delivery systems such as tablets, capsules, ointments etc. show poor bioavailability and plasma level fluctuations and are unable to show sustained release. Without an effective delivery mechanism, the entire therapeutic process may be useless. Maximum efficacy and safety are possible by delivering the drug at a defined controlled rate and to the target site as precisely as possible. The desired system should be able to maintain the optimum concentration of the drug in the blood, to release it in a controlled and targeted manner, and to be able to increase the duration of action of the drug, especially when there is a short duration. Additionally, it should not cause side effects on the patient and avoid frequent doses that lead to a waste of the drug. This kind of delivery systems have numerous advantages in comparison to conventional dosage forms as improved efficacy, reduced toxicity, and improved patient compliance and convenience [56].

Drug release can be described in several different ways:

- *Immediate release* allows drugs to dissolve without the intention of delaying or prolonging dissolution and absorption of the drug,

- *Delayed release* defines the release of the drug at a time other than immediately after administration,

- *Extended release* the products are designed to keep the drug available for an extended period of time after administration,

- *Modified release* includes both delayed-release and extended-release of pharmaceuticals,

- *Controlled release* includes extended release and pulsatile release of drugs,

- *Pulsatile release* assumes the release of finite amounts (or pulses) of the drug at various time intervals that are programmed into the drug product [58].

Control of the drug release can be divided into two independent types, temporal and

distribution control. In temporal control, the drug is protected by an implant/device that can be transported over long distances at certain times of the treatment. This method is applicable to drugs which tend to be rapidly metabolized and eliminated from the body. Temporal control can be achieved by three mechanisms:

1. *Delayed dissolution*

2. *Diffusion controlled release*

3. *Flow control of the drug solution* [59].

In distribution control, the drug delivery system is encapsulated directly to the area where the drug needs to act. Implants suitable for this controlled released system are those which have no harmful side effects for the patient and the drug is unable to exit from the implant. Implantable drug delivery systems (IDDS) are divided into three major categories: biodegradable or non-biodegradable implants, implantable pump systems, and atypical class of implants [59].

In controlled release systems, a well-known phenomenon is the *"burst release"* in which, immediately after placement in the release medium, an initial amount of drug is released before the release rate reaches a stable profile. Burst release leads to a higher initial drug dose and shortens the effective life of the device. It is often considered as an undesirable effect, especially for sustained-release formulations. The burst release can be seen from two perspectives: 1) considered as negative, not desired, since almost the entire drug of interest is released at once, or 2) in some situations rapid release or high initial delivery rate may be desirable. The burst release is unpredictable and cannot be significantly controlled. The most desired release profile allows for a constant rate of drug release, independent of the initial concentration [60, 61, 62].

3.2. Mathematical modelling of drug release

Over the past few decades, several mathematical models, which describe the diffusion and release processes, have been developed and applied to predict the release behaviour over-time of simple and complex drug delivery systems [63, 64]. The benefits of the mathematical modelling result, first, from a more in-depth analysis of the mechanisms controlling drug release from a particular type of dosage form, and second, it is possible to quantify the effect of formulation and processing parameters on the resulting drug release kinetics [65].

Many of the mathematical models that already exist are based on diffusion equations. In the group of major mechanisms controlling drug release are dissolution, diffusion, partitioning, osmosis, swelling and erosion. Drug diffusion is the dominant mechanism in drug delivery and is strongly related to the structure of the material through which the diffusion occurs; therefore, the models must take into account the

morphology of the material alongside other physical factors [9,11].

Diffusion is the movement of a substance from a region of higher concertation to a region of lower concentration. In diffusion controlled released systems, drugs are encapsulated, trapped, and released via diffusion through inert water-insoluble polymeric membranes (reservoir systems) or polymeric matrices (monolithic systems). Diffusion-controlled release systems can be classified into four main types depending on the structure of the systems and the methods of drug delivery:

1. *nonconstant drug source reservoir*

2. *constant drug source reservoir*

3. *monolithic solution*

4. *monolithic dispersion* [59]

3.2.1. Zero order kinetics

Ideal delivery of drugs would follow "zero order kinetics", it is particularly important in certain classes of medicines as antibiotic delivery, heart and blood pressure maintenance, pain control and antidepressants [58].

The velocity of dissolution of the drug from pharmaceutical dosage can be represented by the equation:

$$\frac{dM}{dt} = \frac{DS}{l}(C_s - C) \qquad (3.1)$$

or, simplifying by dividing the volume of the solution V:

$$\frac{dC}{dt} = \frac{DS}{Vl}(C_s - C) \qquad (3.2)$$

where:

M is the mass of solute dissolved during the amount of time;

$\frac{dM}{dt}$ *is the velocity of mass dissolved;*

D is the coefficient of diffusion;

S is the exposed solute area;

L is the thickness of the diffusion layer;

C$_s$ is the solubility of the solid;

C is the concentration of solute in the solvent at time t;

$\frac{dC}{dt}$ *is the velocity of dissolution*

The equation of dissolution is in the simplest form of zero order kinetics model is represented below:

$$W_0 - W_i = K_0 \cdot t \qquad (3.3)$$

where:

W_0 *is the initial amount of drug in solution;*

W_i *is the amount of drug released or dissolved;*

K_0 *is the zero-order release constant.*

Simplifying equation by dividing by W_0 we can get the fraction of solute f_i dissolved in a given time t:

$$f_i = 1 - \frac{W_i}{W_0} = K_0 \qquad (3.4)$$

In this case, we can assume that the tested system is suitable for long-term use for the drug release. The law associated with this system depends on the concentration of the solute C, according to the following equation:

$$C(t) = C_0 + K_0 t \qquad (3.5)$$

On the plot below there is an ideal model of controlled drug release: *cumulative % drug release vs. time* (Figure 15) and an example of graphical representation for zero-order kinetics (Figure 16):
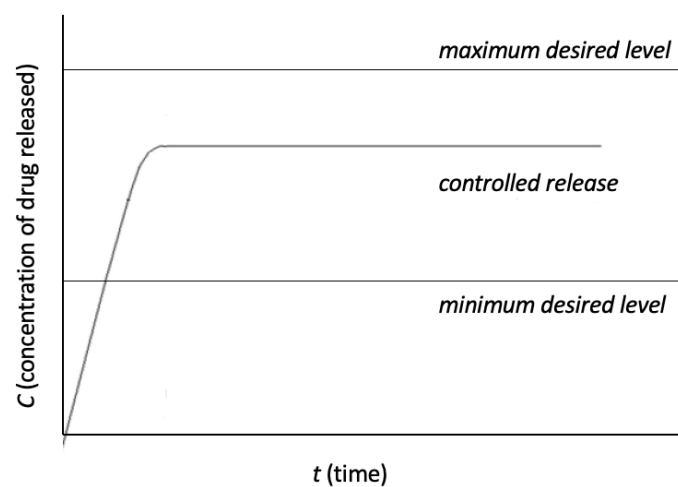
Figure 15: Drug level in the ideal controlled release system with zero-order release kinetics.
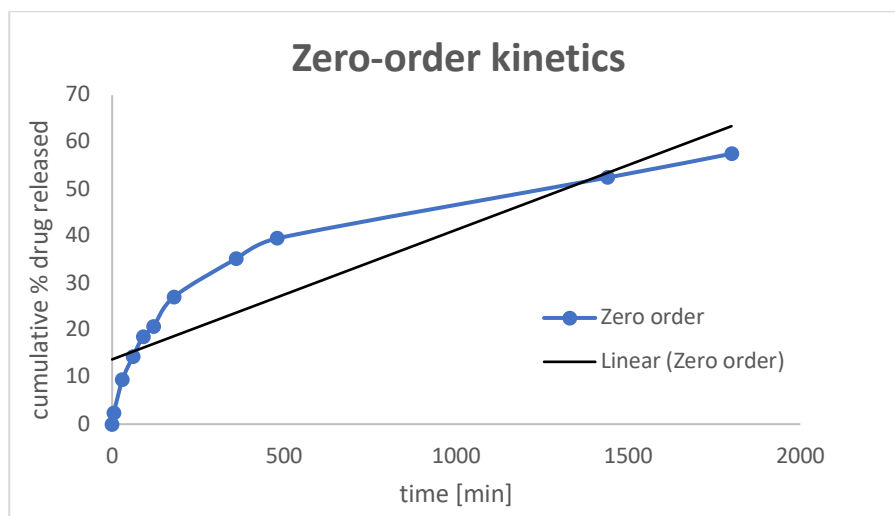
Figure 16: Release profile zero-order kinetics.

3.2.2. First order kinetics

We owe the use of first order kinetics model to Gibaldi and Feldamn (1967) and later to Wagner (1969) who were the first to propose the application of this model for drug dissolution studies. It is a model used to describe the release of several therapeutic agents. This law assumes that the change in the concentration of solute over time depends only on the concentration [66], the release of the drug can be expressed by the equation:

$$\frac{dC}{dt} = -KC \qquad (3.6)$$

where:

K is the first-order release constant;

C is the concentration of pharmaceutical component in the formulation.

Regarding to Noyes and Whitney (1897) the dissolution of a solid particle in a liquid is expressed by the equation:

$$\frac{dC}{dt} = K(C_s - C) \qquad (3.7)$$

where:

t is the time;

C is the concentration;

C_s is the equilibrium solubility for the temperature of the process.

Keeping in mind the available access surface S:

$$\frac{dC}{dt} = K_1 S(C_s - C) \qquad (3.8)$$

Whereas K_1 comes from Fick's first law:

$$K_1 = \frac{D}{Vh} \qquad (3.9)$$

where:

    D is the diffusion coefficient;

    V is the volume of the released drug;

    h is the thickness of the diffusion layer.

Hixson and Crowell made changes to the equation in which the ratio of the solute in a solution is expressed as:

$$\frac{dW}{dt} = KS(C_s - C) \qquad (3.10)$$

and dividing by volume *V*:

$$\frac{dW}{dt} = \frac{KS}{V}(VC_s - W) = k(VC_s - W) \qquad (3.11)$$

where, $k=k_1S$

On the plot below there is an example of drug release with a first order kinetics: Log cumulative % drug remaining vs. time:
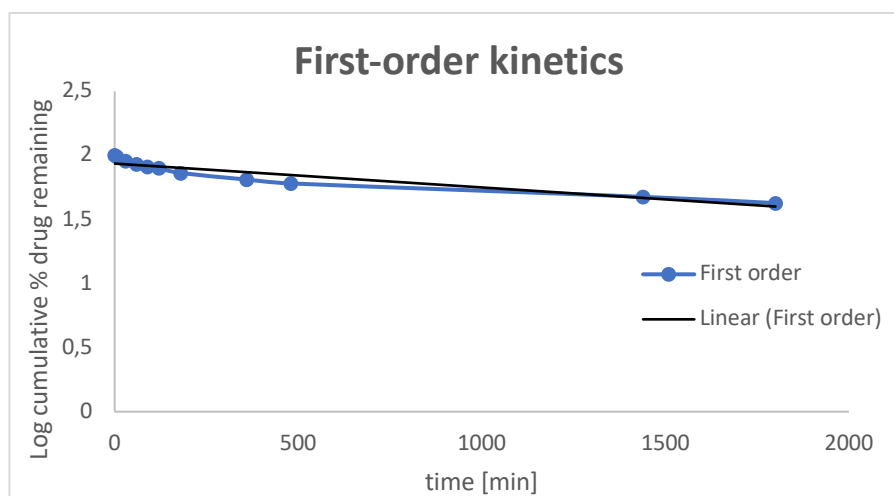
Figure 17: Release profile first-order kinetics.

In 1961 Higuchi was the first to describe a widely used mathematical model of drug released from a matrix system [66]. This model is based on 6 assumptions:

1. *Initial drug concentration in the matrix is much higher than drug solubility.*

2. *Drug diffusion takes place only in one dimension.*

3. *Drug particles are much smaller than thickness of the system.*

4. *Swelling of matrix and dissolution are less or negligible.*

5. *Drug diffusion is constant.*

6. *Perfect sink condition is always achieved in the release environment* [67].

The simplest version of Higuchi's equation takes the form:

$$f_t = Q = K_H \cdot \sqrt{t} \qquad (3.12)$$

where:

K_H is the Higuchi dissolution constant;

f_t is the amount of released drug at time t.

This type of modelling can be used to describe the drug release profile from several types of pharmaceutical dosage forms with modified release, for example some transdermal patches and matrix tablets with water-soluble drugs [66].

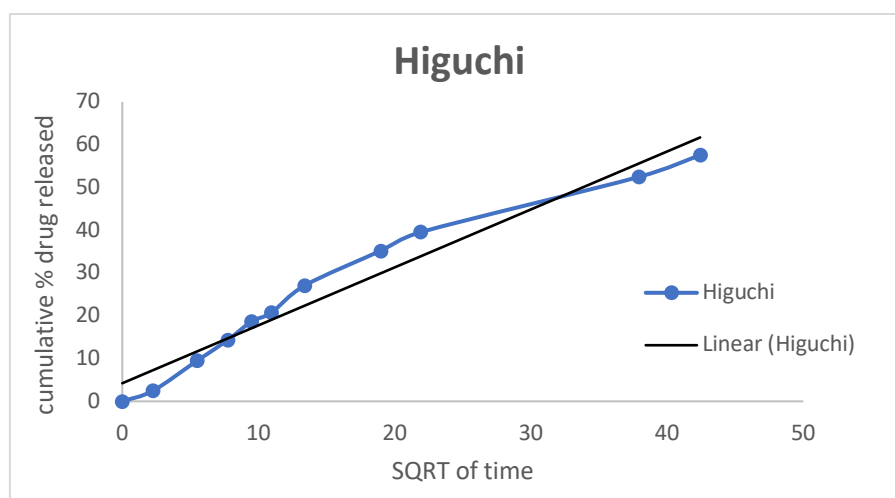A graphical representation of Higuchi modelling of the drug release profile is reported in figure 18:

Figure 18: Release profile Higuchi modelling.

3.2.3. The power law

Another simple and useful equation model is the power law. Used for empirical/semi-empirical mathematical modelling of drug from polymeric layer, derived by Ritger-Peppas and Korsmeyer-Peppas:

$$f_t = \frac{M_i}{M_\infty} = Kt^n \qquad (3.13)$$

where:

f_t is the amount of released drug at time t;

M_∞ is the total amount of encapsulated drug at the equilibrium state;

M_i is the amount of released drug over the time;

t is the time;

K is the constant of release velocity;

n is the exponent of release.

This equation is used to analyse controlled release of water-soluble drugs from the polymers and can be applied to study release profile of hydrophilic drugs.

A graphical representation of Korsmeyer-Peppas modelling for drug release profile:
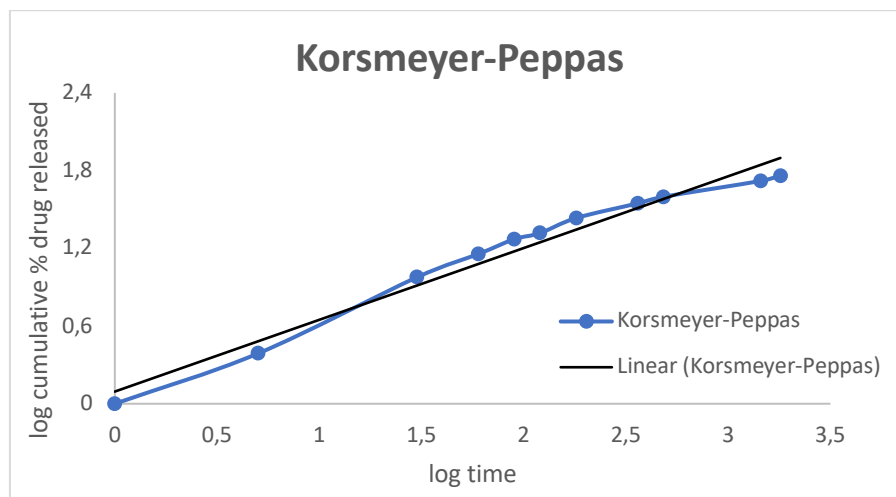
Figure 19: Release profile Korsmeyer-Peppas modelling.

The commonly used power law with the latency time l, which is the start of drug release from the system, the equation is followed:

$$\frac{M_{(i-l)}}{M_\infty} = K(t-l)^n \qquad (3.14)$$

3.2.4. Fickian and Non Fickian diffusion

The process of transport of a drug through a polymer carrier can be well explained by Fick's laws of diffusion, which were derived by Adolf Fick in 1855 [68]. Fick's first law, concerning the assess flux of substances J across virtual interfaces in homogenous solution, is given by the following equation:

$$\frac{1}{A}\frac{dm}{dt} = J = -D\frac{\partial c}{\partial x} \qquad (3.15)$$

where:

    m is the transferred mass;

    A is the area;

    D is the diffusion coefficient;

    c is the concentration;

    $\frac{\partial c}{\partial x}$ *is the concentration gradient.*

Fick's first law assumes that the flux goes from a region of higher concentration to a region of lower concentration. Fick's second law is used for unsteady state situation, when we want to predict how drug concentration changes with time. This law is valid when the amount of the initial drug per unit volume is smaller than the dimensional solubility of drug particle, it assumes that the entire drug dissolves during diffusion process, but that does not apply in the real situations, where there is always some drug left [68]. The diffusion coefficient is seen below:

$$\frac{dc}{dt} = D\frac{d^2 C}{dx^2} \qquad (3.16)$$

Fick's equations can be used to formally derive mathematical models for the analysis in case of diffusion-controlled release processes [69].

From the experimental values, the release exponent n (eq. 3.13-3.14) can be obtained, based on which two classifications can be distinguished: *Fickian and non Fickian* motion.

Fickian and Non Fickian diffusion are two forms of diffusion. The main difference between them is the presence or absence of boundaries.

Non Fickian diffusion refers to the diffusion motion that occurs without obeying Fick's laws of diffusion (anomalous super/sub-diffusion). The following table shows the different types of motion according to the release exponent:

Table 3.1: Diffusion mechanism.

Release exponent (n)	Diffusion mechanism
n < 0.45	Quasi Fickian diffusion
0.45	Fickian diffusion
0.45 < n < 0.89	Anomalous diffusion or Non Fickian diffusion
0.89 – 1	Super Case II relaxation or Non Fickian
n > 1	Non Fickian Super Case II

4 Experimental

4.1. Materials

DL-Menthol (M=157.27 g/mol, racemic ≥ 98.0%, CAS 89-78-1, by Sigma Aldrich, Germany) Thymol (M=150.22 g/mol, ≥ 98.5%, CAS 89-83-8, by Sigma Aldrich, Germany), Ethosuximide (M=141.17 g/mol, CAS 77-67-8, by Sigma Aldrich, Germany), 1,3:2,4-Dibenzylidene D-sorbitol (DBS, > 95%, CAS 32647-67-9, by Accela ChemBio), 3-(Trimethylsilyl)propionic-2,2,3,3-d_4 acid, (TSP, 98 atom % D, CAS 24496-21-8) by Isotec™. Solvents and additives: Distilled water, Deionized water (milliQ water, ultrapure deionized water), PBS (Dulbecco's phosphate-buffered saline tablets, pH 7.2 - 7.6, by Sigma Aldrich, Germany), Deuterium Oxide (99.9 atom % D, CAS 7789-20-0, by Sigma-Aldrich, Germany). All reagents and solvents were used without further purification. The reactions were carried out under atmospheric pressure.

4.2. Material preparation

In the present work, two types of samples were prepared and analysed:

1. Eutectogel loaded with ethosuximide and 5% content of DBS gelator.
2. Eutectogel loaded with ethosuximide and 2% content of DBS gelator.

The preparation of eutectogels started with the preparation of a deep eutectic solvent (DES). Each sample was prepared in the same weight proportions. 0.3 g of menthol and 0.3 g of thymol were weighted, mixed, and heated at about 30-40 ℃ while magnetically stirring until a transparent solution was obtained. The weighted drug - ethosuximide was added to the prepared DES solution. The amount of drug to be loaded varies according to the type of analysis to be performed. The amount of drug for drug release studies was 10 mg; for NMR analysis, two eutectogels with 40 and 100 mg were prepared; for FTIR studies, eutectogels with 100 mg of ethosuximide were prepared. The amount of drug loaded had no effect on the gel preparation steps which started after complete dissolution of the drug.

The gelator amount have been calculated and carefully weighted (5% DBS content and 2% DBS content), all weighted gelator contents are summarized in the table below (Table 4.1). The procedure for preparing eutectogels does not differ depending on the percentage of gelling agent. DBS was added to the vial with the mixture of DES (after the addition of ethosuximide) and heated at about 90-130 ℃ to ensure the gelator dissolution. When the mixture became completely transparent, the contents of the vial were poured into a metal cylinder with a diameter of 1 cm. The prepared eutectogel

was left to solidify and fix the structure during the weekend. In the figure below (Figure 20), it is shown a solidified and ready to analyse eutectogel sample.

Table 4.1: The calculated weights of DBS added to the drug loaded eutectogels.

The amount of ethosuximide			
DBS content	10 mg	40 mg	100 mg
5% DBS	0,0321 g	0,0337 g	0,0368 g
2% DBS	0,0124 g	0,0131 g	0,0143 g

Figure 20: Picture of an eutectogel sample.

4.3. FTIR Experiments

FTIR spectroscopy has been performed on eutectogel samples with and without drug loaded at two different concentration of DBS (2% and 5%) using a Varian 640-IR spectrometer from Agilent Technologies. Eutectogels were prepared according to the procedure described in the paragraph 4.2. The weight of ethosuximide loaded in the eutectogels was equal to 100 mg. The small amount of eutectogel was positioned onto the specific support. Spectra were collected at room temperature in the 400-4000 cm^{-1} wavenumber range, with an average of 64 repetitive scans to guarantee a good signal-to-noise ratio and high reproducibility. The graphs have been displaced in transmittance scale [%] versus wavenumber [cm^{-1}].

4.4. SEM Experiments

Scanning electron microscopy (SEM) was used to analyse the morphology of the prepared eutectogels. Before the analysis, the sample had to be adequately prepared. To do this, menthol and thymol needed to be removed for the gel and replaced with a suitable solvent (ethanol) which could be then evaporated, leaving only the gelator structure. The eutectogels were placed in a glass vial with 10 ml of ethanol, which was

replaced with fresh solution every 30 minutes until no menthol and thymol were left in the structure. In Figure 21 is reported a picture showing the progressive stripping of menthol/thymol from a gel.
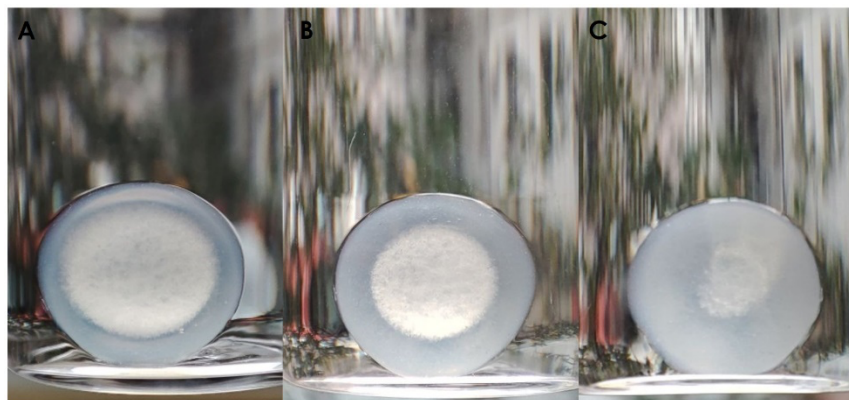

Figure 21: Eutectogel submerged in ethanol for SEM preparation after A) 30 minutes B) 1 hour and C) 2h 30 minutes, close to complete DES removal.

Afterwards, ethanol was removed completely placing the gel on a heating plate at 50°C. This step had to be made carefully in order to avoid sample collapsing when the solvent is removed.

Only eutectogels with 5% DBS content with and without ethosuximide loaded were subjected to SEM experiments. Eutectogels with 2% DBS content collapsed during the preparation steps.

4.5. NMR Experiments

The ^{1}H HR-MAS NMR spectra for eutectogels were recorded on Bruker 500 NEO Spectrometer operating at 500 MHz proton frequency, equipped with a dual ^{1}H/^{13}C HR MAS probe. This instrument produces high resolution quality spectra by using magic angle ($\theta_m = 54.7°$) spinning to remove the line broadening effects caused by dipolar interactions and chemical shift anisotropy. The eutectogels samples were placed in a 4 mm ZrO$_2$ rotor, which contained a volume of about 12 μL. The spinning rate was 4 kHz, and the temperature was stabilized and controlled at 298 K with an air flow of 53 Lh^{-1}.

The diffusion coefficient of the drug and DESs components in gels were measured by diffusion-ordered spectroscopy (DOSY). A sequence of pulses based on bipolar pulse paired, longitudinal eddy-current delay (BPP-LED) was used and a pulse gradient unit was also used to produce magnetic field pulse gradients. The duration of the magnetic field pulse gradients (δ) and the diffusion times (Δ) were optimized and set to $\delta = 3000$

µs, and Δ = 0,4 s. In each experiment, a series of 24 spectra with 16K points were obtained with a D1 relaxation delay of 8s. Each experiment was done in triplicate.

Quantitative NMR (qNMR) experiments were performed to obtain the absolute concentration of a specific compound X from the proton spectrum. This was achieved by adding a known amount of an internal standard to the sample solution and comparing the peaks areas of the compound X to the internal calibration standard. The concentration of the compound X, C_x, in the presence of the calibrant is calculated using the following equation:

$$C_x = \frac{I_x}{I_{cal}} \times \frac{N_{cal}}{N_x} \times C_{cal} \qquad (4.1)$$

where I, N, and C are the integration area, number of nuclei, and concentration of the compound of interest (x) and the calibrant (cal), respectively. In our analyses, the internal standard was TSP at 1.2 mM concentration. The NMR tube preparation consisted of 0,54 μl of the release medium with 0,06 μl of the TSP reference.

The ^{1}H spectra of liquid samples were performed on Bruker 400 Avance Spectrometer. The liquid samples were placed in a 5 mm NMR tube and the ^{1}H spectra were acquired with 16 scans and relaxation delay of 5 s.

4.6. Drug release

- o Eutectogels loaded with ethosuximide were prepared as stated in the material preparation subsection.
- o Preparation of water-based solution PBS buffer: a tablet of phosphate buffered saline was dissolved in around of 500 ml of deionized water. The obtained solution had pH equal to 7.2. To obtain buffer with acidic pH of 4.2, the procedure was repeated with addition of a few drops of hydrochloric acid HCl.
- o Prepared samples were placed in a glass vials with 2 ml of PBS solution as a release medium (see Figure 22).
- o 1 ml of the release medium was collected at specific time intervals and replaced with 1ml of fresh PBS solution.
- o Withdrawal times were set at 5 min, 30 min, 1h, 1h30, 2h, 3h, 6h, 8h, 24 h and 30h. After that PBS was collected every 24h for 18 days (432h).
- o The release experiments were carried out at two different temperatures (room temperature and 37 °C) and at two different pH (7.2 and 4.2). The measurements performed at 37 °C were carried out in a water bath at controlled temperature.
- o Each release experiment has been carried out in triplicate.
- o The table below (Table 4.2) summarizes the names of the tested samples along with the experimental conditions for release.
- o The released medium was analysed using qNMR method and the preparation of the NMR tube is described in the paragraph 4.5.

o Data have been plotted for %mass released versus time [h] as the average of the triplicate measurements.

Table 4.2: The experimental parameters for drug release experiments.

Sample name	Parameters
S1	5% w/w DBS, Room T, pH 7.2
S2	5% w/w DBS, Room T, pH 4.2
S3	5% w/w DBS, T = 37 °C, pH 7.2
S4	5% w/w DBS, T = 37 °C, pH 4.2
S5	2% w/w DBS, Room T, pH 7.2
S6	2% w/w DBS, Room T, pH 4.2
S7	2% w/w DBS, T = 37 °C, pH 7.2
S8	2% w/w DBS, T = 37 °C, pH 4.2

Figure 22: Eutectogels S1 in the release medium.

5 Results

5.1. FTIR analysis

The FTIR analysis was performed on 4 samples, comparing blank eutectogels prepared with 5% w/w and 2% w/w DBS and loaded with the drug in amount of 100 mg. The main spectral region – the hydroxyl stretching region (3000-3700 cm^{-1}) O-H can be seen in all systems, showing the presence of hydrogen bonds forming the gel. The addition of ethosuximide has no noticeable effect on the 5% system (Figure 23). The gel with 2% of DBS, on the other hand, shows some variation of the -OH peak, suggesting that the drug takes part in the hydrogen bond network at low concentration of gelator (Figure 24).
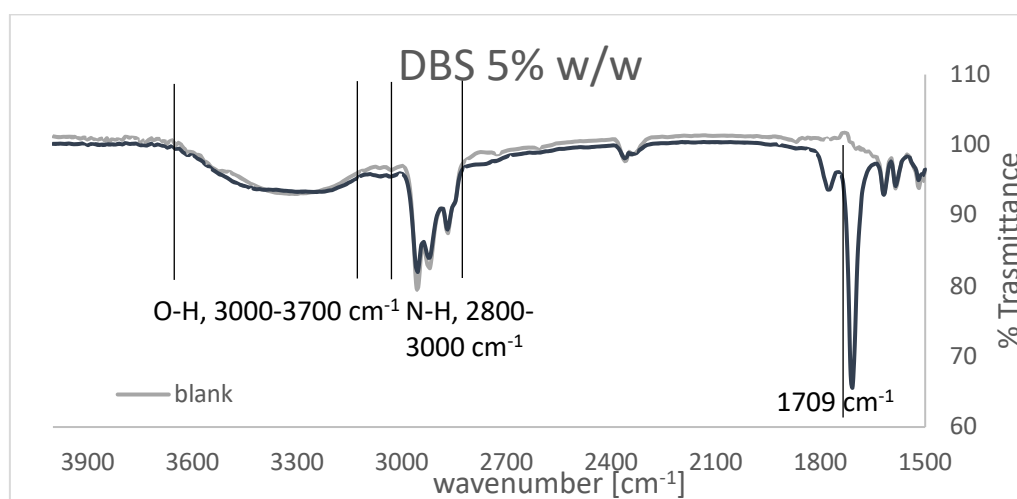
Figure 23: FTIR spectra of eutectogel with 5% w/w DBS.
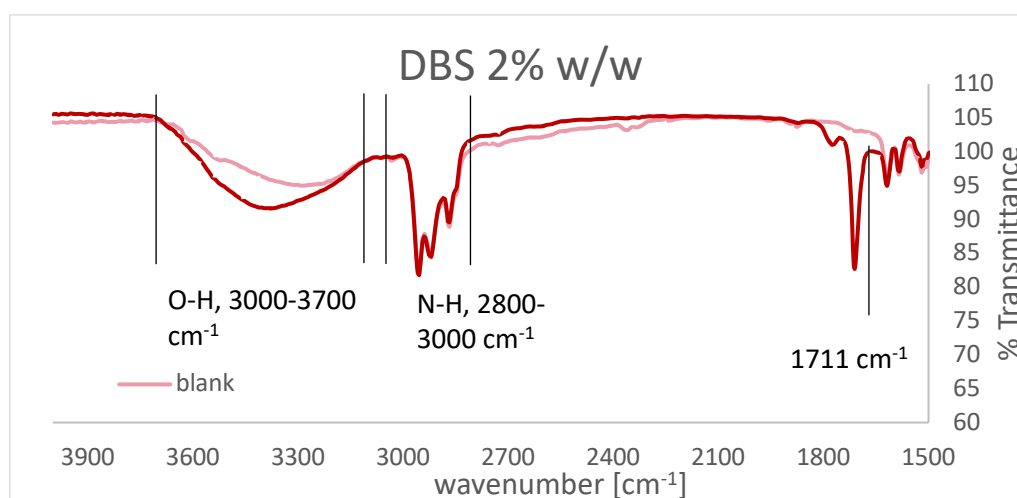
Figure 24: FTIR spectra of eutectogel with 2% w/w DBS.

5.2. SEM analysis

The Scanning electron microscopy images of eutectogels with 5% w/w DBS are reported below. Figure 25 shows the network typically associated to the DBS gelator; in particular, Figure 25A shows blank eutectogel, while Figure 25B eutectogel loaded with ethosuximide.

SEM images show a fibrillar network that is typically formed by molecular gelators, which self-assemble in three-dimensional networks consisting of fibres connected by noncovalent intermolecular interactions such as hydrogen bonding [70]. These non-covalent interactions are also what allow these structures to entrap small molecules within them.
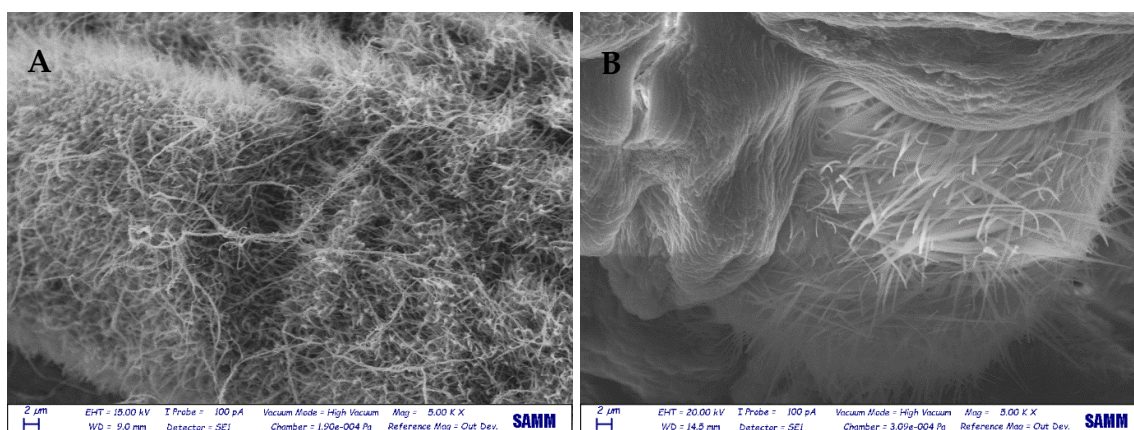
Figure 25: SEM analysis of eutectogel with DBS 5% w/w.

5.3. NMR analysis

This part focused on NMR diffusion analysis of ethosuximide in eutectogels. The figure below (Figure 26) shows the ^{1}H HR-MAS spectra acquired on three different samples. Spectrum A corresponds to the blank eutectogel Men/Thy without drug loaded inside, whereas spectra B and C show eutectogels loaded with 40 mg and 100 mg of ethosuximide, respectively.

In these spectra it is possible observe the different components of the eutectogels, allowing in particular to determine a peak for ethosuximide which is suitable for the analysis of the diffusion measurements. The results of the diffusion studies are reported in figure 27.
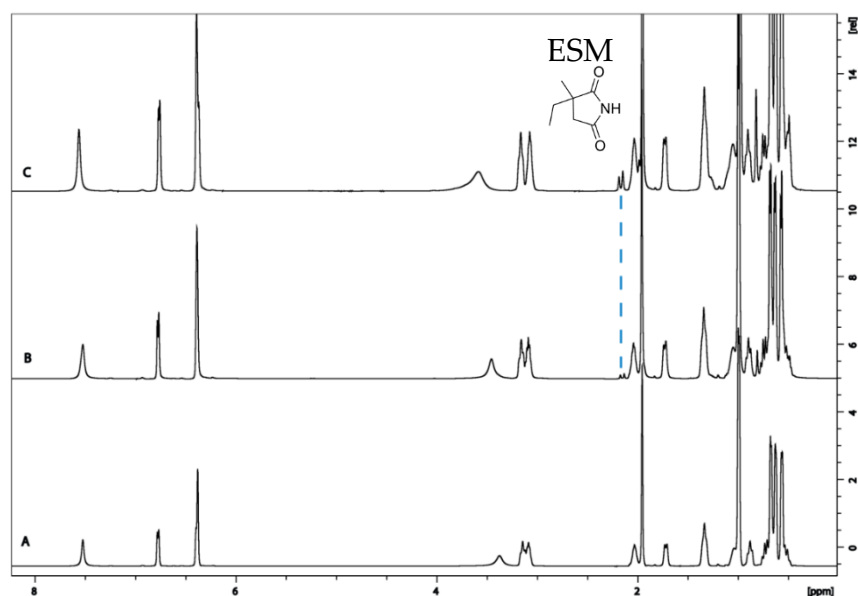
Figure 26: A) ¹H HR-MAS spectrum of blank eutectogel; B) ¹H HR-MAS spectrum of eutectogel with 40 mg Ethosuximide, C) ¹H HR-MAS spectrum of eutectogel with 100 mg Ethosuximide.

Focusing on the behaviour of the drug (Figure 27A) it is first important to notice how the diffusion is slower in the 5% DBS system, as it would be expected considering a more constricted matrix. It is also clear how the diffusion coefficient decreases as the drug concentration increases, in both 2 and 5% DBS systems. This can be associated to the fact that molecules hinder each other's movement as their concentration increases as there is less space for them to move around. This effect is more prominent in the 2% DBS eutectogel as a lower concentration of gelator corresponds to a less entangled fibrillar systems. In 5% DBS gels, ESM molecules exhibit free diffusion, but the variation of the diffusion coefficient with drug concentration, is smaller as the systems is more blocked by the presence of more gelator. From these data it is possible to observe that the effects of the drug and DBS concentration are competitive, but the gelator becomes prominent as its concentration increases.

In addition to the analysis of drug diffusion, it is also interesting to study the behaviour of the DES components (menthol and thymol) since, from HR-MAS NMR measurements it is clear that both these species show a certain mobility inside the gel. Again, the diffusion is slightly faster in the 2 % DBS systems. It is also worthy to notice how the diffusion coefficients of both species has a slightly decreasing trend with the increasing of the drug concentration. Both of these effects are more prominent in the 2% DBS gels, showing again how the increasing strength of the entangled fibrils strongly influences the mobility of small molecules.

The variation of the DES-component diffusion with the drug concentration also seems to support the hypothesis that there is some DES-drug interaction, especially between menthol and ESM, as the $D_{menth} \approx D_{ESM}$ (at 2% DBS and 100 mg of ESM), which could be

explained by the formation of hydrogen bonds between the two species, as also seen in FTIR measurements.
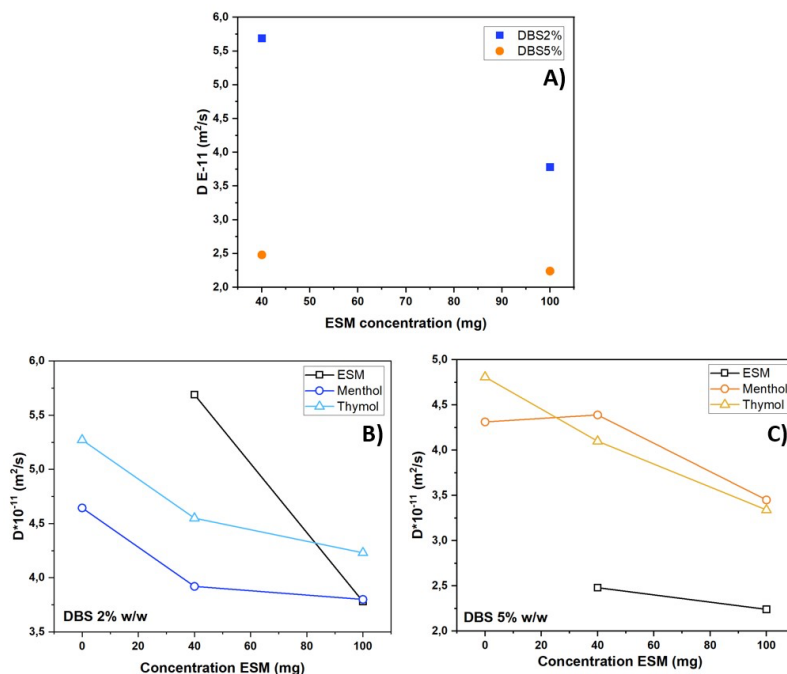

Figure 27: A) Diffusion coefficients of ESM in eutectogels with 2% and 5% DBS. Comparison of diffusion coefficients of DES components and ESM in B) 2% DBS and C) 5% DBS.

The figure below (Figure 28) shows a representative spectrum for the results obtained when testing the release medium with quantitative NMR. The UV-VIS spectrophotometer is the most commonly used method for drug release measurement, however, in this work it was used the quantitative NMR method because it allows for a more specific peak distinction. This ability is shown in the spectrum below: peaks due to different components can be clearly separated, allowing a higher specificity on the drug when analysing the mass released. This was not the case of UV analysis, where all the components had an absorption wavelength in the range of 210-250 nm, making it impossible to clearly separate the different contributions.
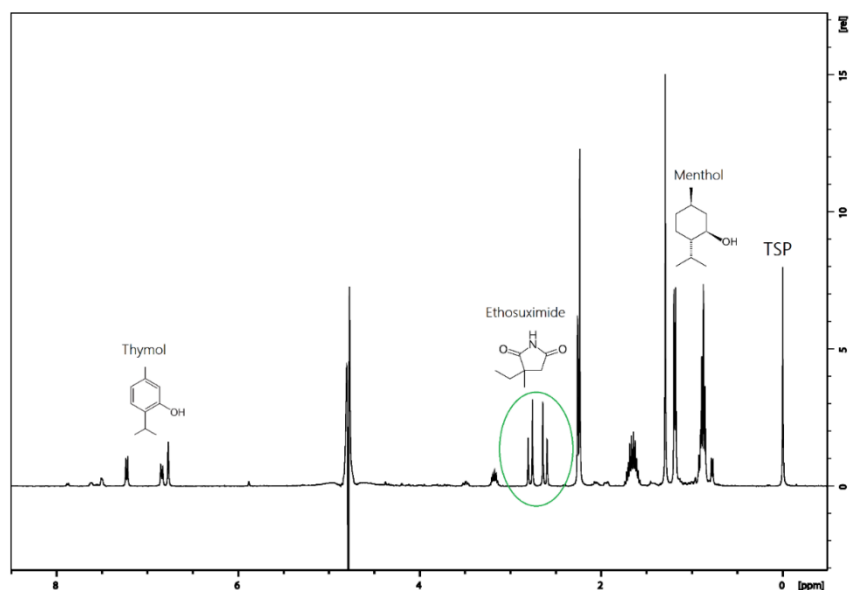
Figure 28: ¹H NMR spectrum of ethosuximide in release medium.

5.4. Drug release profile

Drug release tests have been conducted on the different gel systems, following the protocol described in section 4.6. Drug release profiles are shown in figures 29-34. Overall, for all analysed series, the drug release profiles show an initial burst, which is generally complete within 24 hours. The release of ethosuximide from eutectogel is controlled by the formation of a gel with different contents of DBS gelling agent and varies under different experimental conditions as temperature and pH.

The drug release profiles, obtained at room temperature and pH 7.2 (Figure 29) for 432 hours, show that eutectogel prepared with 2% w/w DBS, releases the drug faster than the gels with 5% DBS. The initial release for two curves overlaps, after 8 hours at 30% of mass released for eutectogel with 2% w/w DBS the release profile starts to be slightly faster than that of 5% w/w. After 18 days 95% of mass release is gained from eutectogels with 2% w/w DBS and 89% from 5% w/w DBS.
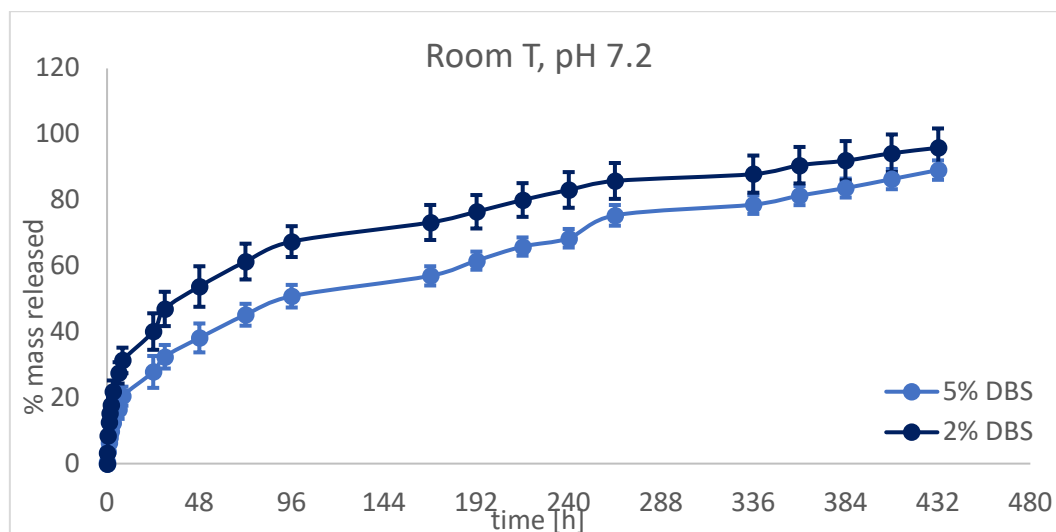
Figure 29: Release profiles of ethosuximide from eutectogels at room temperature and pH = 7.2.

At room temperature and pH 4.2 (Figure 30) a slight change can be observed. For eutectogel with 2% w/w DBS, the drug is released a little faster and after 18 days almost 100% of mass is released, while for eutectogels with 5% w/w DBS the mass released at the same time is about 87%.
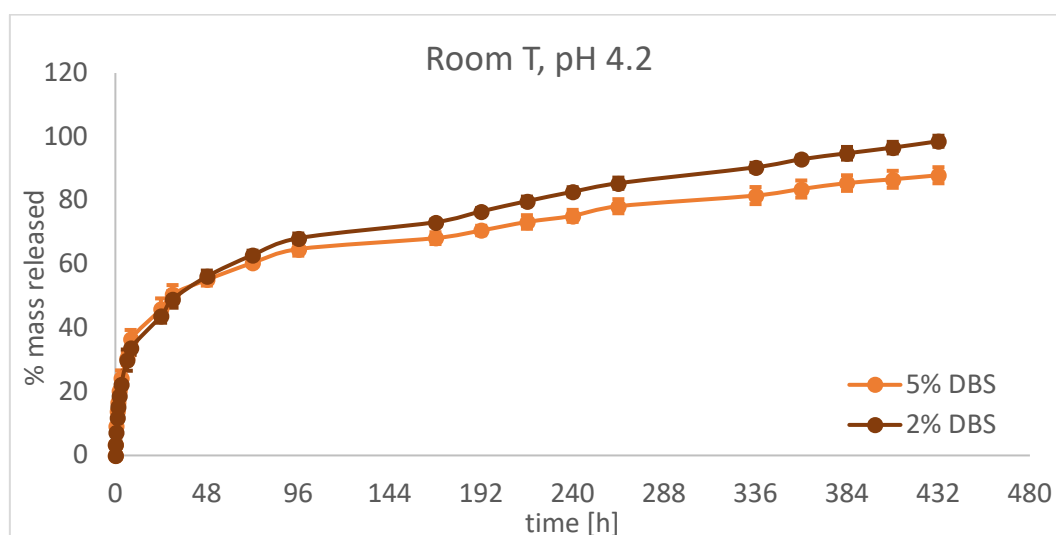

Figure 30: Release profiles of ethosuximide from eutectogels at room temperature and pH = 4.2.

At 37 ℃ and pH 7.2, the drug release process is much faster than at room temperature, the burst effect up to 60% of mass released occurs after 24 hours both from eutectogels with 2% and 5% w/w DBS content. After 18 days both profiles reach almost 100% of mass released.
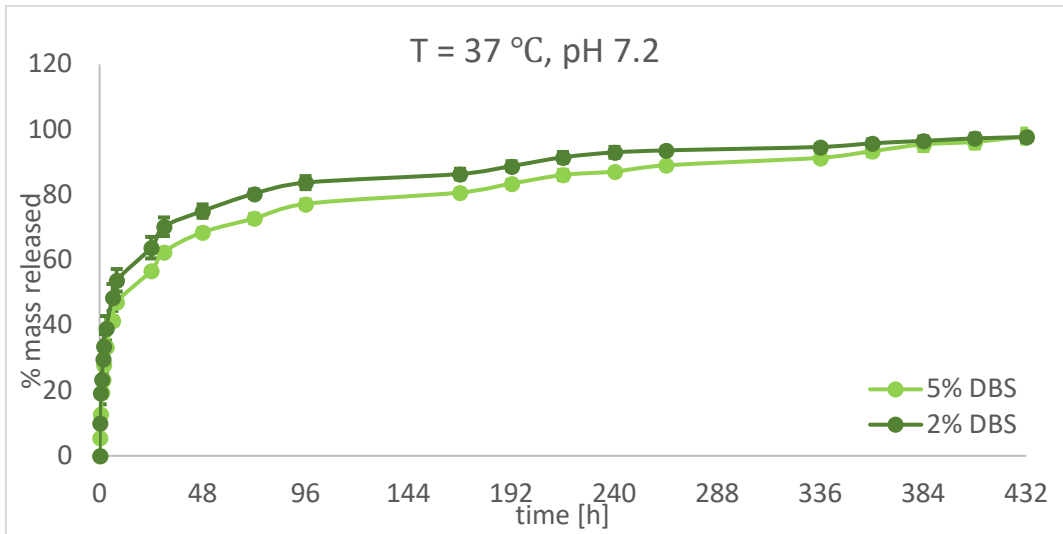
Figure 31: Release profiles of ethosuximide from eutectogels at T = 37 ℃ and pH = 7.2.

In conditions with temperature 37 ℃ and pH 4.2 (Figure 32), the burst effect is reached again after 24 hours, then the amount of drug released slows down to reach 97% and 87% of mass released from eutectogel with 2% w/w and 5% w/w DBS respectively after 18 days. The whole process is slightly faster for eutectogel with 2% DBS content.
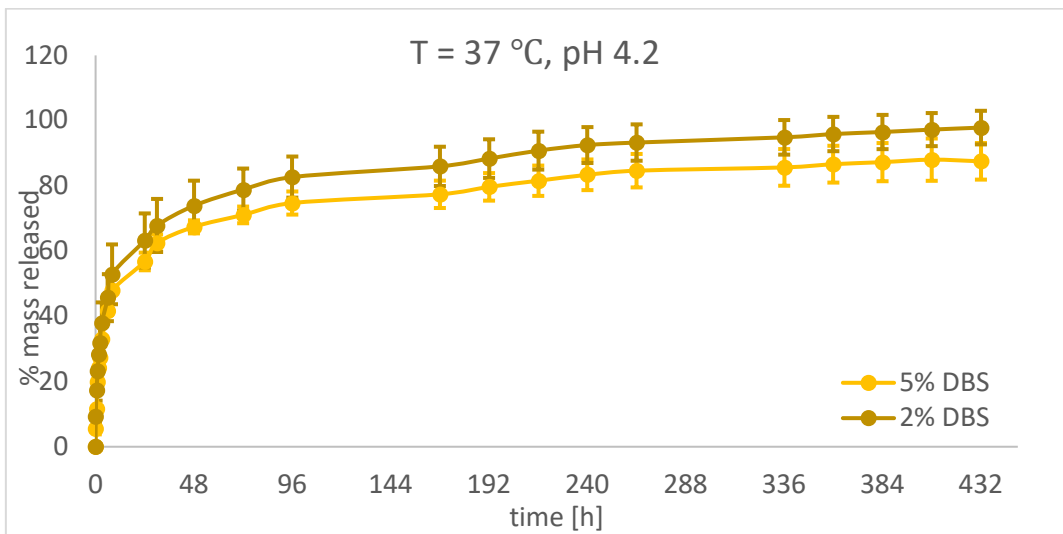

Figure 32: Release profiles of ethosuximide from eutectogels at T = 37 ℃ and pH = 4.2.

Figure 33 below shows all drug release profiles from eutectogels with 5% w/w DBS content under different conditions. The slowest rate of drug release is seen at room temperature and pH 7.2, reaching 89% of mass release after 18 days. At room temperature and pH 4.2, the drug is released faster than for pH 7.2, and after 18 days it reaches 87% of mass released. 100% of mass released is achieved only at 37 ℃, and pH 7.2. The major effect on the release profile is due to the temperature increase.
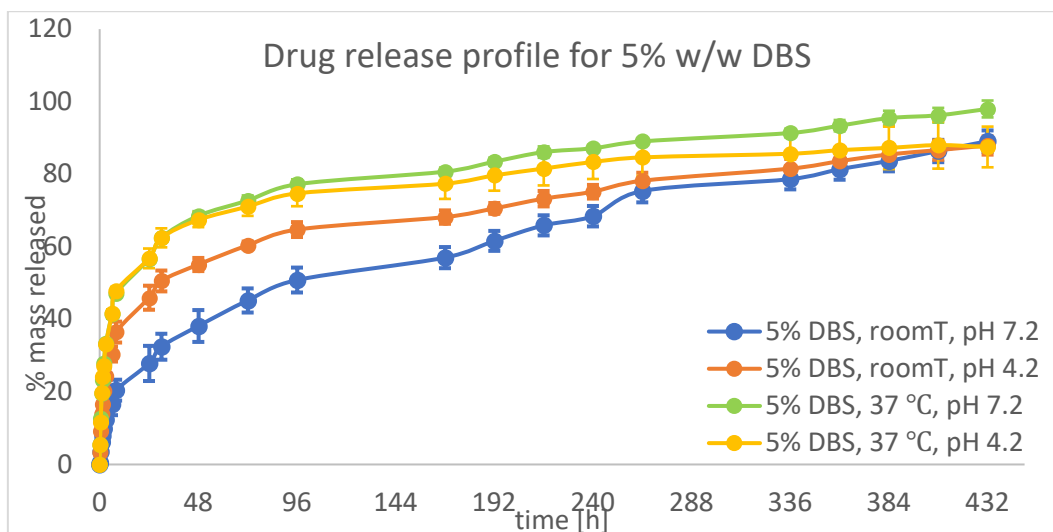
Figure 33: Release profiles of ethosuximide from eutectogels with 5% w/w DBS.

Figure 34 below represents 4 drug release profiles from eutectogels with 2% w/w DBS content under different conditions. The slowest rate of drug release is seen at room temperature and pH 7.2, reaching 95% of mass released after 18 days, for pH 4.2 - 96% of mass released. 100% of mass released is almost achieved in all cases.
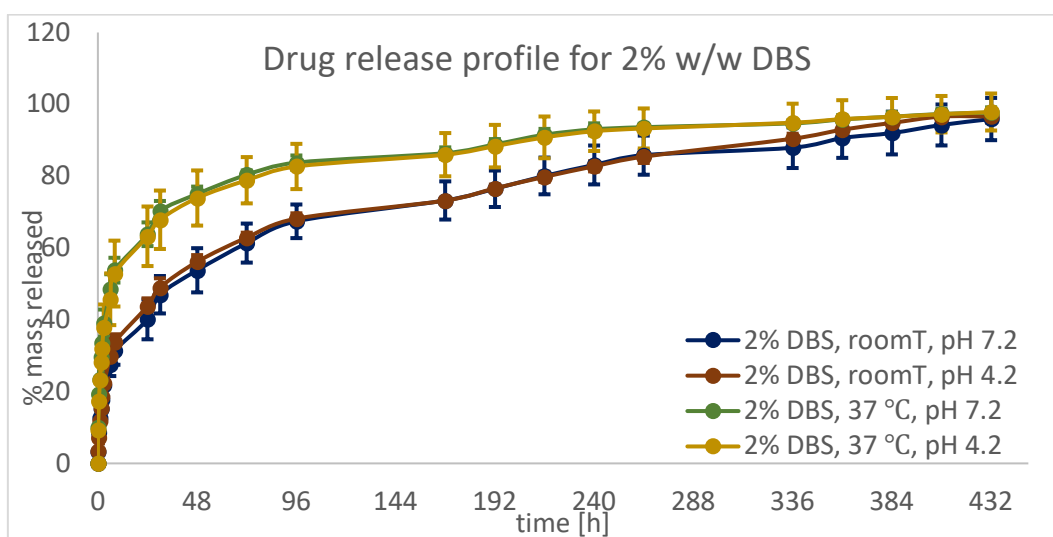

Figure 34: Release profiles of ethosuximide from eutectogels with 2% w/w DBS.

Taking into account the percentage values of the mass released for all analysed cases, it can be concluded that higher values were obtained in the case of eutectogels with a lower content of gelling agent, meaning that the amount of drug released from the

46

eutectogel are affected by the quantity of gelator, as expected. The initial burst released may be correlated to the drug being weakly bonded to the surface of the eutectogels.

It is important to notice how these systems are, in fact, thermo-responsive and pH-responsive, with a slightly different behaviour according to the DBS concentration. In gels prepared with 2% gelator, the main effect seems to come from the temperature variation, as the burst release is always faster at 37°C. The variation of pH, on the other hand, does not seem to affect too much the release profile.

The response of the gels prepared with 5% DBS seems more variable: again, the higher effect comes from the temperature as higher temperatures equal faster releases rates. It is also possible to see some effect of the pH in this case, especially for the room temperature-pH 4.2 condition, where the release is faster than the correspondent room temperature-pH 7.2. This could be related to the fact that an acidic environment influences the strength of hydrogen bonds, weakening them and allowing a higher mobility of the species entrapped in the fibrillar system. It would be interesting to study the effect of pH at even higher acidities, such as 1.2 for example, to gain a better understanding of its effect on the hydrogen bond system.

5.5. Mathematical modelling

Useful information on release mechanisms is obtained by mathematical modelling of drug release profiles. To better understand the mechanism of release from eutectogels, the experimental ESM release profiles (up to 60% cumulative release) for all eutectogel formulations were fitted using different kinetic models including: zero order kinetics, first order kinetics, Korsmeyer-Peppas, and Higuchi. Table 5.1 presents the results for all 4 models together with the correlation coefficient (R^2). The R^2 values are in the range of 0.65-0.99. The best results were obtained for the Korsmeyer-Peppas model (all with R^2 in the range of 0.98-0.99), therefore this method was chosen to analyse the drug release mechanism as the most precise and accurate method.

Table 5.1: The summarized values for the correlation coefficient (R^2) for mathematical modelling.

	Zero order kinetics	First order kinetics	Korsmeyer-Peppas	Higuchi
	R^2	R^2	R^2	R^2
S1	0.8257	0.9055	0.9957	0.9741
S2	0.7163	0.7997	0.9898	0.9279
S3	0.6532	0.7567	0.9861	0.9075
S4	0.6509	0.7529	0.9841	0.9053
S5	0.8162	0.8902	0.9933	0.9623

S6	0.7942	0.8717	0.9925	0.9562
S7	0.8172	0.8988	0.9960	0.9774
S8	0.8255	0.8255	0.9957	0.9801

Table 5.2: summarizes the fitting results for the Korsmeyer-Peppas model with the constant K and the diffusion exponent n, indicative of the drug transport mechanism. For all samples analysed the values of n are less than 0.45 indicating a quasi-Fickian diffusion mechanism for ethosuximide released from both eutectogel formulations.

Table 5.2: The summarized values of the correlation coefficient (R^2), K constant and n the diffusion exponent.

Korsmeyer-Peppas modelling		
R^2	K	n
S1 0.99578609	0.05907786	0.21648865
S2 0.98984493	0.04329311	0.32133957
S3 0.98611717	0.07676123	0.27523084
S4 0.98416317	0.07624857	0.27703054
S5 0.993306755	0.112286876	0.159019423
S6 0.992591687	0.11662362	0.157776563
S7 0.996077418	0.097476336	0.264075568
S8 0.995777539	0.092021791	0.268003356

Figure 35 shows the eight graphs corresponding to the fit of all release studies (up to 60%) with the Korsmeyer-Peppas model. Two lines were drawn, the blue line corresponding to the experimental results and the orange line to the fit.
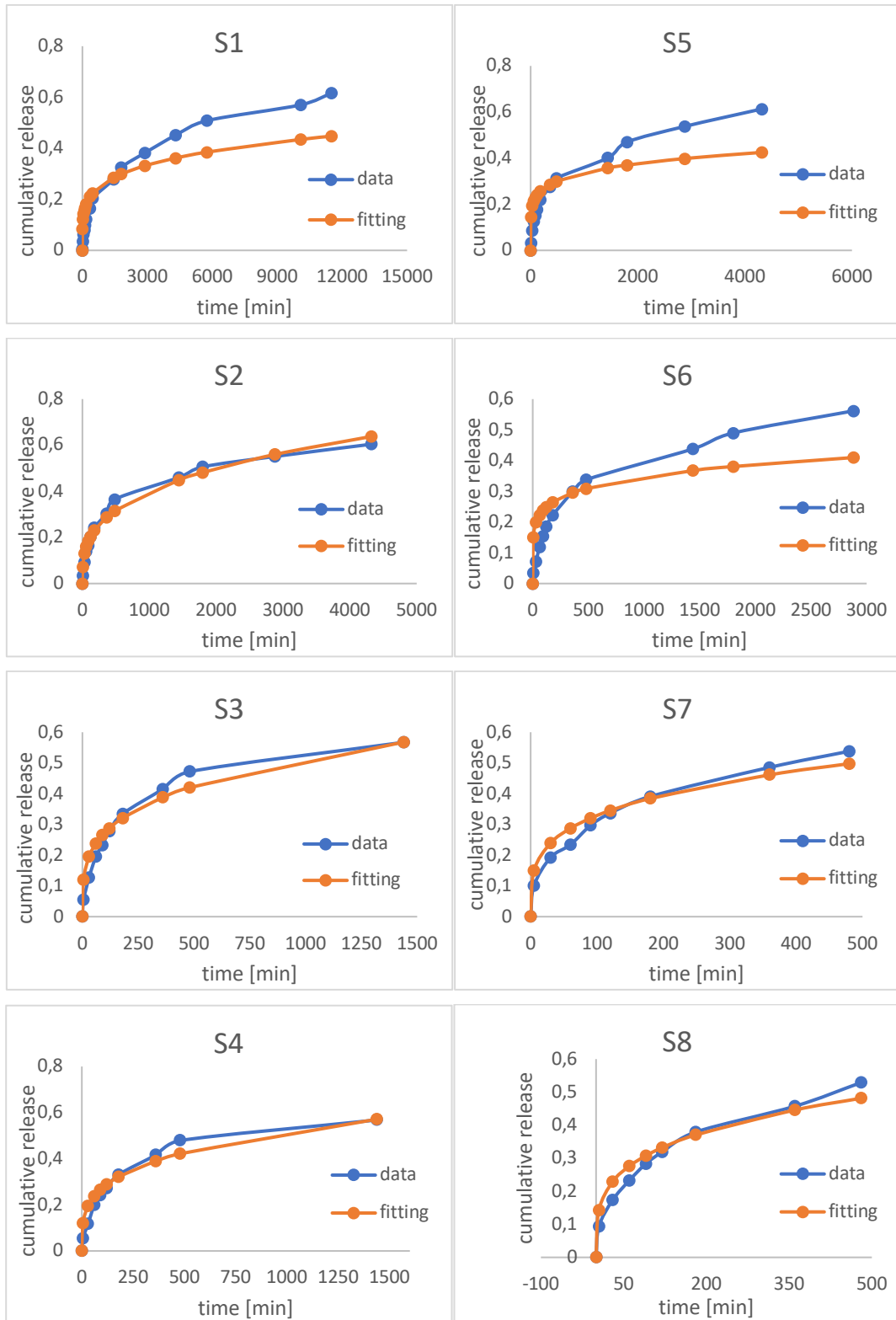
Figure 35: Korsmeyer-Peppas model fitting for the samples S1-S8.

6   Conclusions and future developments

The purpose of this work was to develop novel physical gels based on type V deep eutectic solvents (menthol-thymol) as drug delivery systems. The gels, loaded with ethosuximide anti-epileptic drug, were prepared through an easy, low-cost four steps procedure. Two types of gels were prepared by varying the amount of the DBS gelator added. The morphology and structure of these gels were investigated by SEM and FT-IR techniques. Moreover, ^{1}H HR-MAS NMR methods are used to study, at the molecular level, the dynamics of the drug molecules in the gel network. The results clearly show the complexity of the non-covalent interactions between menthol-thymol and the drug molecules within the entangled structure imposed by the DBS gelator. In particular, obtained NMR data highlighted the presence of menthol-drug hydrogen bonds which play a relevant role in drug solubilisation and diffusion motion. Finally, *in vitro* release profiles were explored in different pH (7.2 and 4.2) and temperature (room temperature and 37° C) experimental conditions. The results demonstrated the ability of all eutectogels formulations to release ethosuximide for up to three weeks with a dual thermo- and pH- responsiveness, proving that the different environments influence the strength of hydrogen bonds, weakening them and allowing a higher mobility of the molecules entrapped in the fibrillar systems. Much better results with faster release of the drug were obtained at a temperature of 37 °C, which confirmed the possibility of use in the human body, whose temperature is equal to 36.6 °C. For the two different pHs, neutral and acidic, there is some difference in the mass released for the gel prepared with the highest DBS amount, in acidic conditions the release is slightly faster, and it could be correlated to the influence of acidic environment in the strength of hydrogen bonds. Considering these results, it could be interesting to analyse the drug release profile at even higher acidities, such as pH=1.2 for example, to gain a better understanding of its effect on the hydrogen bond network.

Furthermore, the weight percentage of the gelling agent used during the eutectogels preparation influences the rate of drug release. Among the two weight contents (2% and 5%) used, significantly faster release of the drug was obtained for the lower content of DBS. This may be due to the fact that lower gelling agent content results in a less entangled structure of the eutectogel network, and thus the gel may be more susceptible to various external conditions to release the drug. All the release profiles were fitted with the Korsmeyer-Peppas mathematical model which indicated that the release mechanism is driven by quasi-Fickian diffusion.

The obtained results allow the conclusion that eutectogels can be a new class of drug delivery systems, but further in-depth analysis and research are necessary. Moreover, in the future, research could focus on how increasing the content of the gelling agent affects the release of the drug and the 3D network of the eutectogels.

In this work, only one drug was used – ethosuximide, which is widely used as an anticonvulsant, but in the future, it will be interesting to analyse the release of other active pharmaceutical ingredients with different properties for the treatment of other diseases.

Bibliography

[1]   A. P. Abbott, G. Capper, D. L. Davies, R. K. Rasheed and V. Tambyrajah, "Novel solvent properties of cholibe chloride/urea mixtures," *Chemical Communications*, no. 1, pp. 70-71, 2003.

[2]   B. B. Hansen, A. Horton, B. Chen, D. Poe, Y. Zhang, S. Spittle, J. Klein, L. Adhikari, T. Zelovich, B. W. Doherty, B. Gurkan, E. Maginn, A. Ragauskas, M. Dadmun, T. Zawodzinski and G. A. Baker, "Deep Eutectic Solvents: A Review of Fundamentals and Applications," 2020.

[3]   S. Emami and A. Shayanfar, "Deep eutectic solvents for pharmaceutical formulation and drug delivery applications," *Pharmaceutical Development and Technology*, 2020.

[4]   S. N. Pedro, C. S. Freire, A. J. Silvestre and M. G. Freire, "Deep Eutectic Solvents and Pharmaceuticals," *Encyclopedia*, no. 1, pp. 942-963, 2021.

[5]   B. B. Hansen, S. Spittle, B. Chen, D. Poe, Y. Zhang, J. M. Klein, A. Horton, L. Adhikari, T. Zelovich, B. W. Doherty, B. Gurkan, E. J. Maginn, A. Ragauskas, M. Dadmun and T. Zawodzinski, "Deep Eutectic Solvents: A Review of Fundamentals and Applications," *Chemical Reviews*, vol. 121, pp. 1232-1285, 2021.

[6]   L. Lomba, C. B. Garcia, M. P. Ribate, B. Giner and E. Zuriaga, "Applications of Deep Eutectic Solvents Related to Health, Synthesis, and Extraction of Natural Based Chemicals," *Applied Sciences*, no. 11, 2021.

[7]   X. Ge, C. Gu, X. Wang and J. Tu, "Deep eutectic solvents (DESs)- derived advanced functional materials for energy and environmental applications: challenges, opportunities, and future vision," *Journal of Materials Chemistry A*, no. 5, 2017.

[8]   R. T. Sekharan, M. R. Chandira, S. Tamilvanan, S. Rajesh and B. Venkateswarlu, "Deep Eutectic Solvents as an Alternate to Other harmful Solvents," *Biointerface Researcg in Applied Chemistry*, vol. 12, no. 1, pp. 847-860, 2022.

[9]   M. A. Martins, S. P. Pinho and J. A. Coutinho, "Insights into the Nature of Eutectic and Deep Eutectic Mixtures," *Journal of Solution Chemistry,* vol. 48, pp. 962-982, 2019.

[10] Y. Liu, J. B. Friesen, J. B. McAlpine, D. C. Lankin, S.-N. Chen and G. F. Pauli, "Natural Deep Eutectic Solvents: Properties, Applications, and Perspectives," *Journal of Natural Products,* no. 81, pp. 679-690, 2018.

[11] M. A. Martins, S. P. Pinho and J. A. Coutinho, "Insights into the Nature of Eutectic and Deep Eutectic Mixtures," *Journal of Solution Chemistry,* vol. 48, pp. 962-982, 2019.

[12] T. E. Achkar, H. Greige-Gerges and S. Fourmentin, "Basics and properties of deep eutectic solvents: a review," *Environmental Chemistry Letters,* vol. 19, pp. 3397-3408, 2021.

[13] D. A. Alonso, A. Baeza, R. Chinchilla, G. Guilena, I. M. Pastor and D. J. Ramon, "Deep Eutectic Solvemts: The organic Reaction Medium of the Century," *European Journal of Organic Chemistry,* pp. 612-632, 2016.

[14] D. Machon, P. Toledano and G. Krexner, "Phenomenological theory of the phase diagrams of binary eutectic systems," *Physical Review B,* no. 71, 2005.

[15] C. M. Chabib, J. K. Ali, M. A. Jaoude, E. Alhseinat, I. A. Adeyemi and I. M. Al Nashef, "Application of deep eutectic solvents in water treatment processes: A review," *Journal of Water Process Engineering,* vol. 47, 2022.

[16] M. H. Zainal-Abidin, M. Hayyan, G. C. Ngoh, W. F. Wong and C. Y. Looi, "Emerging frontiers of deep eutectic solvents in drug discovery and drug delivery systems," *Journal of Controlled Release,* 2019.

[17] A. R. C. Duarte, A. S. D. Ferreira, S. Barreiros, E. Cabrita, R. L. Reis and A. Paiva, "A comparison between pure active pharmaceutical ingredeints and therapeutic deep eutectic solvents: Solubility and permeability studies," *European Journal of Pharmaceutics and Biopharmaceutics,* no. 114, pp. 296-304, 2017.

[18] A. Roda, F. Santos, A. A. Matias, A. Paiva and A. R. C. Duarte, "Design and processing of drug delivery formulations of therapeutic deep eutectic systems for tuberculosis," *The Journal of Supercritical Fluids,* no. 161, 2020.

[19] I. M. Aroso, R. Craveiro, A. Rocha, M. Dionisio, S. Barreiros, R. L. Reis, A. Paiva and A. R. C. Duarte, "Design of controlled release systems for THEDES -

Therapeutic deep eutectic solvents, using supercritical fluid technology," *International Journal of Pharmaceutics*, no. 492, pp. 73-79, 2015.

[20] W. Lu and H. Chen, "Application of deep eutectic solvents (DESs) as trace level drug extractants and drug solubility enhancers: State-of-the-art, prospects and challenges," *Journal of Molecular Liquids*, vol. 349, 2022.

[21] S. Emami and A. Shayanfar, "Deep eutectic solvents for pharmaceutical formulation and drug delivery applications," *Pharmaceutical development and technology*, 2020.

[22] E. L. Smith, A. P. Abbott and K. S. Ryder, "Deep Eutectic Solvents (DESs) and Their Applications," *Chemical Reviews*, no. 114, pp. 11060-11082, 2014.

[23] G. Di Carmine, A. P. Abbott and C. D'Agostino, "Deep eutectic solvents: alternative reaction media for organic oxidation reactions," *Reaction Chemistry & Engineering*, vol. 6, no. 582, 2021.

[24] S. N. Pedro, M. G. Freire, C. S. Freire and A. J. Silvestre, "Deep eutectic solvents comprimising active pharmacutical ingredients in the development of drug delivery systems," *Expert opinion on drug delivery*, 2019.

[25] Y. Liu, Y. Wu, J. Liu, W. Wang, Q. Yang and G. Yang, "Deep eutectic solvents: Recents advances in fabrication approaches and pharmaceutical applications," *International Journal of Pharmaceutics*, vol. 622, 2022.

[26] C. V. Pereira, J. M. Silva, L. Rodrigues, R. L. Reis, A. Paiva, A. R. C. Duarte and A. Matias, "Unevil the Anticancer Potential of Limonene Based Therapeutic Deep Eutectic Solvents," *Scientific Reports nature research*, vol. 9, 2019.

[27] G. P. Kamatou, I. Vermaak, A. M. Viljoen and B. M. Lawrence, "Menthol: A simple monoterpene with remarkable biological properties," *Phytochemistry*, 2013.

[28] J. M. Silva, C. V. Pereira, F. Mano, E. Silva, V. I. Castro, I. Sa-Nogueira, R. L. Reis, A. Paiva, A. A. Matias and A. R. C. Duarte, "Therapeutic Role of Deep Eutectic Solvents Based on Menthol and Saturated Fatty Acids on Wound Healing," *ACS Applied Bio Materials*, no. 2, pp. 4346-4355, 2019.

[29] I. A. Freires, C. Denny, B. Benso, S. M. de Alencar and P. L. Rosalen, "Antibacterial Activity of Essential Oils and Their Isolated Constituents against Cariogenic Bacteria: A Systematic Review," *Molecules*, no. 20, pp. 7329-7358, 2015.

[30] A. Escobar, M. Perez, G. Romanelli and G. Blustein, "Thymol bioactivity: A review focusing on practical applications," *Arabian Journal of Chemistry,* no. 13, pp. 9243-9269, 2020.

[31] M. F. Nagoor Meeran, H. Javed, H. Al Taee, S. Azimullah and S. K. Ojha, "Pharmacological Properties and Molecular Mechanisms of Thymol: Prospects for Its Therapeutic Potential and Pharmaceutical Development," *Frontiers in Pharmacology,* vol. 8, 2017.

[32] M. C. Martinez-Pabon and M. Ortega-Cuadros, "Thymol, menthol and eucalyptol as agents for microbiological control in the oral cavity: A scoping review," *Rev. Colomb. Cienc. Quim. Farm,* vol. 49, no. 1, pp. 44-69, 2020.

[33] S. Shiyab, M. Shatnawi, R. Shibli, M. Al-Zweiri, M. Akash and T. Aburijai, "Influence of development stage on yield and composition of Origanum syriacum L. oil by multivariate analysis," *Journal of Medicinal Plants Research,* vol. 6, no. 15, pp. 2985-2994, 2012.

[34] S. V. Chamundeeswari, E. J. Jebaseelan Samuel and N. Sundaraganesan, "Quantum mechanical and spectroscopic (FT-IR, FT-Raman, 13C, 1H and UV) investigations of antiepileptic drug Ethosuximide," *Spechrochimica Acta Part A: Molecular and Biomolecular Spectroscopy,* no. 83, pp. 478-489, 2011.

[35] S. R. Benbadis, R. G. Beran, A. T. Berg, J. Engel Jr., A. S. Galanopoulou, P. W. Kaplan, M. Koutroumanidis, S. L. Moshe, D. R. Nordli, J. M. Serratosa, S. M. Sisodiya, W. O. Tatum IV and T. Valeta, "Ethosuximide," in *Atlas of Epilepsies,* Springer-Verlag London Limited, 2010.

[36] K. Sommerfeld-Klatta, B. Zielińska-Psuja, M. Karaźniewicz-Łada and F. K. Główka, "New Methods Used in Pharmacokinetics and Therapeutic Monitoring of the First and Newer Generation of Antiepileptic Drugs (AEDs)," *Molecules,* vol. 25, 2020.

[37] H. Zhang, N. Tang, X. Yu, M.-H. Li and J. Hu, "Strong and Though Physical Eutectogels Regulated by the Spatiotemporal Expression of Non-Covalent Interactions," *Advanced Functional Materials,* 2022.

[38] J. Ruiz-Olles, P. Slavik, N. K. Whitelaw and D. K. Smith, "Self-Assembled Gels formed in Deep Eutectic Solvenys - Supramolecular Eutectogels with High Ionic Conductivities," *Angewandte Chemie International Edition,* pp. 4173-4178, 2019.

[39] J. Wang, S. Zhang, Z. Ma and L. Yan, "Deep eutectic solvents: progress and challenges," *Green Chemical Engineering,* vol. 2, pp. 359-367, 2021.

[40] D. J. Mercurio, S. A. Khan and R. J. Spontak, "Dynamic rheological behavior of DBS-induced poly(propylene glycol_ physical gels," *Rheol Acta,* vol. 40, pp. 30-38, 2001.

[41] B. O. Okesola, V. M. Vieira, D. J. Cornwell, N. K. Whitelaw and D. K. Smith, "1,3:2,4-Dibenzylidene-D-sorbitol (DBS) and its derivatives - efficent, versatile and industrally - relevant low-molecular-weight gelators with over 100 years of history and a bright future," *Soft Matter,* vol. 11, 2015.

[42] J. B. Lambert and E. P. Mazzola, Nuclear Magnetic Resonance Spectroscopy An Introduction to Principles, Applications, and Experimental Methods, Pearson Education.

[43] J. Keeler, Understanding NMR Spectroscopy, James Keeler, University of Cambridge, 2002.

[44] X. Liu, Organic Chemistry I, Kwantlen Polytechnic University, 2021.

[45] J. C. Edwards, "Principles of NMR," Process NMR Associates LLC, Danbury.

[46] W. S. Price, "Pulsed-Field Gradient Nuclear Magnetic Resonance as a tool for studying translational diffusion: part 1, basic theory," *Magnetic Resonance,* vol. 9, no. 5, pp. 299-336, 1997.

[47] W. Maas, F. Laukien and D. Cory, "Gradient High Resolution, Magic Angle Sample Spinning NMR," *Journal of American Chemical Society,* vol. 118, pp. 13085-13086, 1996.

[48] P. Mazzei and A. Piccolo, "HRMAS NMR spectroscopy applications in agriculture," *Chemical and Biological Technologies in Agriculture,* vol. 4, no. 11, 2017.

[49] H. Farooq, D. Courtier-Murias, R. Soong, W. Bermel, W. M. Kingery and A. J. Simpson, "HR-MAS NMR Spectroscopy: A Practical Guide for Natural Samples," *Current Organic Chemistry,* vol. 17, pp. 3013-3031, 2013.

[50] A. Wong and C. Lucas-Torres, "High-resolution Magic-angle Spinning (HR-MAS) NMR Spectroscopy," *The Royal Society of Chemistry,* pp. 133-150, 2018.

[51] T. Alam and J. Jenkins, HR-MAS NMR Spectroscopy in Material Science, London: IntechOpen, 2012.

[52] F. Ocampos, L. Menezes, L. Dutra, M. Santos, S. Ali and A. Barison, "NMR in Chemical Ecology: An Overview Highlighting the Main NMR Approaches," *eMagRes,* vol. 6, pp. 325-342, 2017.

[53] B. C. Smith, Fundamentals of Fourier Transform Infrared Spectroscopy, Boca Raton: CRC Press, 2011.

[54] K. Wagatsuma, Spectroscopy for Materials Analysis An Introduction, Singapore: Springer Verlag, 2021.

[55] L. Reimer, Scanning Electron Microscopy Physics of Image Formation and Microanalysis, Berlin, Heidelberg: Springer, 2010.

[56] K. E. Uhrich, S. M. Cannizzaro, R. S. Langer and K. M. Shakesheff, "Polymeric Systems for Controlled Drug Release," *Chemical Reviews,* 1999.

[57] M. Saltzman, "Introductory Material: Introduction," in *Drug Delivery Engineering Principles for Drug Therapy,* Oxford University Press, 2001, p. 5.

[58] G. Singhvi and M. Singh, "Review: In vitro drug release characterization models," *International Journal of Pharmaceutical Studies and Research,* vol. 2, no. 1, pp. 77-84, 2011.

[59] C. T. Huynh and D. S. Lee, "Controlled Release," *Encyclopedia of Polymeric Nanomaterials,* 2014.

[60] O. Evrova and J. Buschmann, "In vitro and in vivo effects of PDGF-BB delivery strategies on tendon healing: A review," *European Cells and Materials,* vol. 34, pp. 15-39, 2017.

[61] X. Huang and C. S. Brazel, "On the importance and mechanisms of burst release in matrix-controlled drug delivery systems," *Journal of Controlled Release,* vol. 73, pp. 121-136, 2001.

[62] S. Bhattacharjee, "Understanding the burst release phenomenon: toward designing effective nanoparticulate drug-delivery systems," *Therapeutic Delivery,* 2020.

[63] A. Elmas, G. Akyuz, A. Bergal, M. Andac and O. Andac, "Mathematical modelling of drug release," *Research on Engineering Structures & Materials,* vol. 6, no. 4, pp. 327-350, 2020.

[64] N. A. Peppas and B. Narasimhan, "Mathematical models in drug delivery: How modelling has shaped the way we design new drug delivery systems," *Journal of Controlled Release,* vol. 190, pp. 75-81, 2014.

[65] J. Siepmann and F. Siepmann, "Modelling of diffusion controlled drug delivery," *Journal of Controlled Release,* vol. 161, pp. 351-362, 2012.

[66] S. Dash, P. N. Murthy, L. Nath and P. Chowdhury, "Kinetic modelling on drug release from controlled drug delivery systems," *Acta Poloniae Pharmaceutica - Drug Research,* vol. 67, pp. 217-223, 2010.

[67] K. Ramteke, P. Dighe, A. Kharat and S. Patil, "Mathematical Models of Drug Dissolution: A Review," *Scholars Academic Journal of Pharmacy (SAJP),* vol. 3, no. 5, pp. 388-396, 2014.

[68] R. Awasthi, V. K. Pawar and G. T. Kulkarni, "Controlled Release and Gastroretentive Drug Delivery Systems".

[69] C. Mircioiu, V. Voicu, V. Anuta, A. Tudose, C. Celia, D. Paolino, M. Fresta, R. Sandulovici and I. Mircioiu, "Mathematical Modeling of Release Kinetics from Supramolecular Drug Delivery Systems," *Pharmaceutics,* vol. 11, no. 140, 2019.

[70] A. Singh, F.-I. Auzanneau, M. G. Corradini, G. Grover, R. G. Weiss and M. A. Rogers, "Molecular Nuances Governing the Self-Assembly of 1,3:2,4-Dibenzylidene-d-sorbitol," *Langmuir,* vol. 33, pp. 10907-10916, 2017.

List of Figures

List of Tables